Mobilization and Immobilization of Repository-Related Trace Elements in Granitic Rocks

Kurt Mengel

Technische Universität Clausthal
Institut für Mineralogie und Mineralische Rohstoffe
Fachgebiet Mineralogie-Geochemie-Salzlagerstätten

November 2001

Acknowledgement:

The underlying work of this report was supported by the Federal Ministry of Economics and Technology (BMWi) under the identification number 02 E 8916. Responsibility for the contents of this publication lies solely with the authors.

Contents

Abstract

In an attempt to investigate the retention capacity of granites with respect to repository-related elements, the mobilization and immobilization of chemical elements within the granite is studied by detailed geochemical analyses of fresh and intensively altered rocks from the Äspö region (SE Sweden). In addition, the specific retention of repository-related elements in epidote is studied by an experimental approach in which Th-, U-, and REE-enriched solutions were equilibrated with epidote at elevated temperatures.

Among the repository-related elements, Fe, Co, Ba, and LREE were originally mobilized on a cm- to dm-scale but have subsequently been immobilized *in-situ* by incorporation into secondary minerals. The mineral epidote, which is present in all altered granites, can take up REE, U, and Th from hydrothermal solutions. Taking Ce as natural analogues for actinides (Np, Pu, Am), the distribution of Ce Th, U extrapolated to temperatures of 50 to 100^{o}C reveals a strong uptake of these elements from hydrothermal solutions (*D*-values of 8 to 1512).

The main results obtained from the analysis of a one km^3 reference volume and from experimental element partitioning can be applied to an assumed granite volume of $5 \cdot 10^7$ m^3, which is heated to 50^{o}C by heat transfer from buried spent fuel. The retention capacity of Fe, Co, Y, Sr, Cs, Ba, and REE in the granitic matrix volume is derived from the reduction of the results obtained for a one km^3 reference volume. The retention capacity of epidote for REE, U, and Th is derived from the application of experimentally established *D*-values to the matrix volume assuming low water/rock ratios and ambient temperatures of 50^{o}C. The matrix volume assumed here contains 5 modal % of epidote.

The combined retention capacities of repository-related elements under realistic assumptions result in a nearly complete immobilization of Fe, Co, Ba, REE, Th, Np, and of more than 85 % of the Pu and Am contained in 8000 t of spent fuel. The highly mobile elements Sr and Cs are probably not immobilized from migrating underground solutions. It is concluded that epidote-bearing granites of a heated matrix volume may serve as an effective geological barrier for a number of repository-related elements contained in spent fuel.

1. The project in the context of the German Research and Development Scheme for nuclear waste repositories

The German government provides funds for research and development in the field of high-level waste (spent fuel) disposal in deep geological formations. In addition to the investigations of rock salt as a potential host rock formation, research activities are also focused on hard rocks.

With respect to their suitability as host rocks, granitic rocks reveal a number of distinct features when compared with rock salt. The latter is practically dry, shows plastic behavior and is generally isolated from aquifers of the sedimentary cover. Rock salt may behave as a nearly perfect geological barrier system. However, it does not possess any significant immobilization capacities for spent fuel-relevant chemical elements. Granitic rocks, on the other hand, behave brittle upon low-temperature deformation, are extensively intersected by fissures and fractures and are thus open to the circulation of groundwater. In contrast to evaporites, granites do have significant immobilization capacities as a result of water/rock interactions occurring at post-magmatic temperatures. Thus, granites certainly are not ideal geological barriers from the viewpoint of rock mechanics and hydrology, but they may very well immobilize spent fuel-relevant elements from migrating underground solutions.

The aim of this project is the study of the immobilization capacity of granitic rocks. The various research activities focusing on the mobilization and immobilization of repository-related elements are part of the BMWi research program for the disposal of hazardous waste in deep geological formations (PTE 1998). Based on the philosophy that a proper understanding of geological processes of the past will help to extrapolate similar behavior in the future, the project contributes geochemical evidence to the current discussion about the safety of potential repository sites in granitic formations.

Granites are the most abundant rocks of the upper 20 km of the continental crust. Viewed from a global perspective, they have been formed by common geological processes. The chemical and petrological composition of granites in Europe is fairly homogeneous. Thus, results obtained from one specific site are generally transferable to other granite formations.

2. Connections with SKB activities

Svensk Kärnbränslehantering AB (SKB) has designed the Äspö Hard Rock Laboratory (HRL) to meet the needs of research and development for the final disposal of spent nuclear fuel in granitic rocks. In addition, the HRL provides the opportunity to test methods for the characterization of selected repository sites.

The rock masses surrounding a repository are supposed to constitute a natural barrier to prevent radionuclides from entering the biosphere. The most important property of the natural barrier is seen in its ability to protect the technical barriers from unwanted reactions with migrating solutions, thus providing stable chemical and mechanical conditions for a minimized transport of radionuclides.

Among the numerous research activities carried out by SKB in the HRL, the project reported here is related to the **T**racer **R**etention **U**nderstanding **E**xperiments (TRUE), which are designed to better understand the radionuclide retention in the rock. SKB's experimental program is designed to create a data base for the conceptual and numerical modeling on different scales. The TUC project on the mobilization and immobilization of trace elements in the geological barrier was not part of the TRUE program, but the results may provide independent evidence for the behavior of granitic rocks in terms of an irreversible fixation of radionuclides in granite minerals. Following the TRUE approach, which is designed to work on a laboratory (dm) to block scale range (several tens of meters), the TUC project envisages a larger scale in order to take account of the large-scale lithological heterogeneities of the Äspö granitoids.

The experimental approach of the TUC project deals with the potential incorporation of repository-related elements in natural minerals at elevated temperatures, which may occur in the area surrounding emplaced canisters. Since the rock volume, heated to 50 - 100°C, is rather small when compared to the bulk mass of the geological barrier, a one km^3 reference volume of granite has been employed here.

3. Introduction and objectives

Any model of deep repository of spent nuclear fuel in granitic rocks should include detailed investigations of the geochemical and mineralogical composition of the granites and their interaction with migrating fluids in the geological past. Geochemical analyses of natural processes in the past are the key to a) understanding the distribution of chemical elements in such rocks and in hydrous fluids and b) predicting the migration of elements contained in nuclear waste due to possible mobilization from leaking canisters in the future. Reactions between rock-forming minerals and migrating fluids enriched in radionuclides from leaking canisters also can be predicted for temperatures ≤100^{o}C on the basis of experimentally derived partitioning coefficients. An experimental technique is employed here to characterize the retention capacity of specific minerals (epidote/allanite) with respect to radionuclides using REE as a natural analogue.

The chemical composition of a granitic body - as it is exposed today - is the result of three major geological processes: (i) solidification of a silicate magma intruding into the earth's upper crust at shallow levels (2 to 10 km depths); (ii) high-temperature alteration (400 to 600^{o}C) of the rock by hydrous fluids released from the solidified rock volume; (iii) low-temperature-reaction of metastable high-temperature silicates with hydrous fluids at temperatures around and below 100^{o}C. Because the stages of hydrothermal alteration events may occur episodically and continue over several tens of millions of years, such reactions are capable of causing chemical redistributions of mobile elements on a grain size as well as on a meter to tens-of-meter scale.

The completely solidified magma formed at stage (i) contains high temperature silicates (plagioclase, quartz, alkali feldspar, biotite, hornblende) which cannot take up elements with very large ionic radii and high field strength in their lattice in large quantities. During hydrothermal reactions at temperatures around 400^{o}C, minerals like epidote and titanite are formed. They contain noticeable amounts of REE, Th, U and other elements that do not fit into the crystal structures of the magmatic phases. At the high-temperature alteration stages all minerals are formed by chemical components which originate from *inside* the granitic body. In contrast, low-temperature alteration is generally caused by influx of hydrous fluids from *outside* the granite. The extent and degree of low-temperature reaction is determined by the water/rock ratio and the secular availability of fluids from external sources. The secondary minerals formed at this stage are epidote, chlorite, muscovite, prehnite, kaolinite, and zeolites. These minerals have very interesting properties with respect to the retention of elements that occur as long-lived radionuclides in nuclear waste. It is predicted that a number of trace elements will be retained in secondary minerals upon reaction with migrating underground solutions. Thus, the low-temperature reaction products represent a potential sink for mobilized radionuclides.

Natural rocks do not contain any actinides besides Th and U. As a basis for the study of the geochemical behavior of heavier actinides, the REE which are present in all granitic rocks at low concentration levels between about 0.5 and 100 ppm are taken as natural analogues. REE have a number of geochemical similarities compared with actinides in terms of their ionic

radii, valence state and complexation characteristics.

The main objectives of the research project reported here are summarized below. They are subdivided into two major aspects:

1. Mass balance for gain and loss of repository-related trace elements during the geological past and principles of their redistribution within a reference volume of Äspö granitoids.
2. Retention of repository-related elements in epidote-bearing granites at temperatures up to 100°C.

Combining the evidence derived from the geochemical investigations of fresh and altered granites in a large volume with the distribution coefficients obtained for epidote-bearing granites at elevated temperatures yields a fairly complete image of the immobilization capacities of the geological barrier granite for selected repository-related elements.

The analytical procedures include information on the methods employed, whose accuracy and precision are described in the Appendix (Chapter A1). Details of the experimental determination of the epidote/allanite partition coefficients (*D*-values), such as the starting material (epidote and synthetic trace element-enriched solutions), are given in Chapter A4 of the Appendix.

4. Characterization of Äspö granitoids

4.1. Petrography and alteration stages

A detailed petrographic description of the Äspö granitoids investigated here is summarized in the Appendix (Chapter A2). The dominant rock types in the Äspö area are granitoids varying in composition from granites *sensu stricto* via diorites, quartz-monzonites to monzonites. Previous surface mapping (Kornfält and Wikman, 1987) has led to a classification of the granitic rocks as Fine-grained Granite, Ävrö Granite and Småland Granite. For the underground mapping of the HRL-tunnel, a more detailed classification scheme has been established by Munier (1995). His classification scheme, consisting of Fine- and Medium-grained Granites, Småland Granites and Äspö Diorites, has been adopted here (see Tab. 1). According to the tunnel mapping data presented in Tab. 1, the other rock types in the Äspö area, known as 'greenstones' (amphibole-rich basites) and 'metavolcanics' (meta-andesites and meta-dacites) as well as mylonites, make up less than 5 % of the total rock mass. Since these rock types do genetically not belong to the granitoid series, they will not be taken into account any further.

Tab. 1: Distribution of the different rock types in the HRL-tunnel (Munier, 1995).

Rock type	Volume proportions [%]
Äspö Diorite	47
Småland Granite	35
Fine- and Medium-grained Granite	13
Other rock types (Green-stones etc.)	5

4.2 Classification of rock alteration

Four stages of alteration which have modified the primary magmatic mineral assemblages have been identified here. In the nearly unaltered samples (**stage I**) rare signs of alteration, if they are present at all, can be observed in K-feldspar and biotite. Plagioclase exhibits slightly turbid zones along twinning planes. In the altered samples (**stage II** and **III**) biotite is partly transformed into chlorite plus secondary titanite and rutile, and primary plagioclase is partly (II) or nearly completely (III) decomposed to the secondary assemblage albite, epidote, calcite and muscovite. The complete alteration of all main mineral phases results in **stage IV** altered rocks, where all minerals except quartz are characterized by a complete breakdown of primary magmatic assemblages into the secondary minerals stated above. The mineral allanite was found in 6 samples. This mineral has grown at the expense of epidote by reaction with hydrothermal fluids. A summary of this classification scheme is given in Tab. 2.

Tab 2. Classification of Äspö granitoids based on the alteration state of constituent minerals

	Alteration state of constituent minerals		
Alteration stage	Plagioclase	Alkali feldspar	Biotite
I	Fresh to slightly altered	Fresh	Fresh
II	Partly altered	Slightly altered	Slightly altered
III	Near completely altered	Slightly altered	Partly altered
IV	Completely altered	Altered	Completely altered
IV*	Alteration similar to IV plus additional calcite and epidote veins		

4.3 Volume distribution of the main granitoid types

For the calculation of net gains and losses produced by hydrothermal reactions it is necessary to establish a data base for the volume distribution of the major Äspö rock types. The total amount of chemical elements mobilized by water/rock interaction during the geological past will be calculated by comparison of very fresh and strongly altered granites. Such mass balance calculations require the assumption of a rock mass in which the respective alteration and mobilization reactions have occurred. This rock mass should be significantly larger than the individual rock masses of fresh and strongly altered rocks and should not be much larger than the volume of granite supposed to be affected by the deposition of waste containers. For this reason, a reference volume of one km^3 has been chosen. This reference volume is assumed to meet the above-mentioned requirements and will thus be taken to serve as an appropriate precondition on which the mass balance calculations are to be based.

For a representative one km^3 reference-block of Äspö granitoids, the volume distribution of the main Äspö granitoid types was adopted from the data base of Markström and Erlström (1996) and the tunnel mapping of Munier (1995). To integrate these data into the classification scheme of alteration given here, the „fresh granites“ in Markström and Erlström (1996) have been assigned to alteration stages I and II and those described as ‘chloritisized’ and/or ‘oxidized’ to alteration stages III and IV. The relative distribution of rock types observed in the Äspö area is used to calculate the mass distribution employing the density data given by Stanfors et al. (1994). The results are summarized in Tab. 3.

Tab. 3: Volume- and mass-distribution of the three main granitoids in the Äspö-region.

	One km^3 reference block		
Rock type	Volume portion [Vol. %]	Volume [km^3]	Mass [10^9 t]
Äspö Diorite, fresh	42.60	0.43	1.17
Äspö Diorite, altered	6.59	0.07	0.18
Småland Granite, fresh	31.61	0.32	0.84
Småland Granite, altered	5.31	0.05	0.14
Fine-/Medium-grained Granite, fresh	12.58	0.13	0.34
Fine-/Medium-grained Granite, altered	1.31	0.01	0.03

4.4 Chemical redistributions in whole rocks

The spatial distribution of granitoid samples of alteration stage I through IV is very close, e.g. strongly altered Äspö Diorites occur very close to fresh portions of this rock type. The reason is probably the existence of former alteration zones which are assumed to be related to extinct fractures or fissures within the granite massive. To check for local mobilization and immobilization on a 1 dm^3 scale (the scale of whole-rock samples investigated) it is useful to compare very fresh with significantly altered material taken from adjacent outcrops in the tunnel or from individual drill cores. Tab. A2 in the Appendix shows chemical data of selected Äspö granitoids as examples of very fresh (stage I) to altered (stage II and IV) samples. The chemical differences between fresh and altered rock types are much less pronounced than the differences between the granitoid types themselves; e.g. the SiO_2 values of fresh and altered samples vary within the analytical error, whereas the Småland Granites and Äspö Diorites have much lower silica contents when compared to Fine- and Medium-grained Granites. This observation holds for the majority of elements analyzed with the exception of some alkali and alkaline-earth elements.

With some rare exceptions, for all elements analyzed here the chemical variability within each rock type is significantly lower than the differences between samples located close together shown in Tab. A2. Hence, it is concluded that the mobilization of elements observed on a sample size scale was followed by fixation of the mobilized elements almost in their place of origin. This implies that the majority of mobilized material has not migrated very far within the rock volume but rather was immobilized by *in-situ* formation of new secondary mineral assemblages as observed in alteration stage II and IV rocks.

However, the chemical variability observed within the suite of rock samples investigated is not only due to hydrothermal reactions but was also caused by primary magmatic processes such as melt differentiation in magma chambers in the course of solidification. In order to distinguish between the magmatic and the hydrothermal processes it is necessary to clarify the effects of magmatically induced chemical variations.

4.5 Magmatic versus hydrothermal chemical variations

The rock types from Äspö cover a wide range of major element concentrations. This compositional range is due to differentiation processes inherited from the magmatic stages of their formation. The compositional variation within fresh Äspö Diorite, Småland Granites and Fine- to Medium-grained Granites is plotted in TiO_2-based diagrams. Titanium behaves completely immobile during all types of hydrous and hydrothermal rock alterations and, furthermore, serves as a very good indicator of chemical variations triggered by magmatic processes. Fig. 1 shows the compositional variation in fresh and altered rock types in TiO_2-based diagrams. Many elements show correlations with TiO_2 either as a positive or a negative slope of the regression line of fresh rock types. The regression line is calculated exclusively from unaltered samples and the dotted lines include the element variations exclusively caused by magmatic processes. Any data points outside the field between the dotted lines are thus due to post-magmatic hydrothermal alteration reactions. Data points above the dotted lines indicate gains and those below the dotted lines losses. The largest deviations from the magmatic trend lines are observed for Na, K, Ca, Rb and Sr, whereas those of Si, Al, Fe, Mg, and P are comparatively small. SiO_2, Al_2O_3, MnO, MgO and P_2O_5 reveal no systematic deviation from either preferred gain or loss. There seems to be a specific loss for Ca and Sr, and for K and Rb a specific gain.

For the majority of the trace elements investigated here, the concentrations in Äspö granitoids vary over 3 orders of magnitude. Therefore, they cannot be plotted in conventional SiO_2- or TiO_2-based diagrams. To solve this problem and also for the sake of clarity, these trace element concentrations have instead been normalized to average contents in the continental crust and to average chondrites (REE), respectively (see Fig. 2 and Fig. 3).

In Fig. 2, the range of unaltered granitoids from Äspö is shown as a gray area, the altered varieties are plotted as individual data points connected by lines. Similar to the observation made for major elements in Fig. 1, there are very few strongly altered samples which show distinct deviations from the magmatically induced variations. Small gains or losses are observed for the extremely mobile alkali elements Li and Cs. U, Th, Hf, and Y plot within the magmatic variation field. The deviation of Hf in two samples of altered Äspö Diorite is probably not caused by hydrothermal mobilization. In granitic rocks, Hf is fixed almost exclusively in the mineral zircon ($ZrSiO_4$), and small variations in the modal abundance of zircon will result in relatively large deviations from the magmatic trend lines. Therefore, the low Hf contents in Äspö Diorites are not regarded as significant.

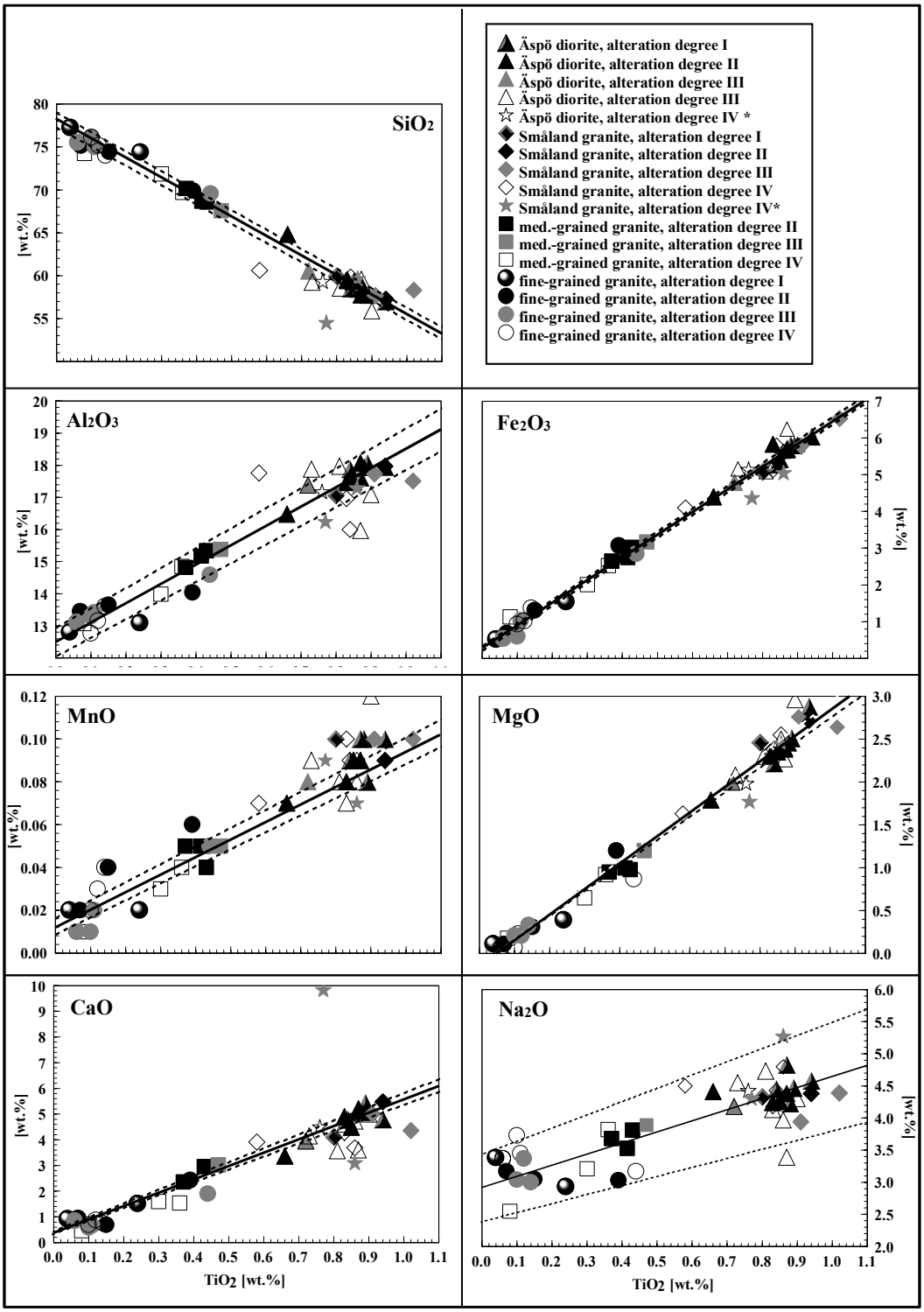

Fig. 1: Major element variation of fresh and altered Äspö granitoids. The solid line is a linear regression through alteration-type I granitoids and represents the magmatic variability; dashed lines indicate the upper and lower limit of chemical variations within unaltered rock species.

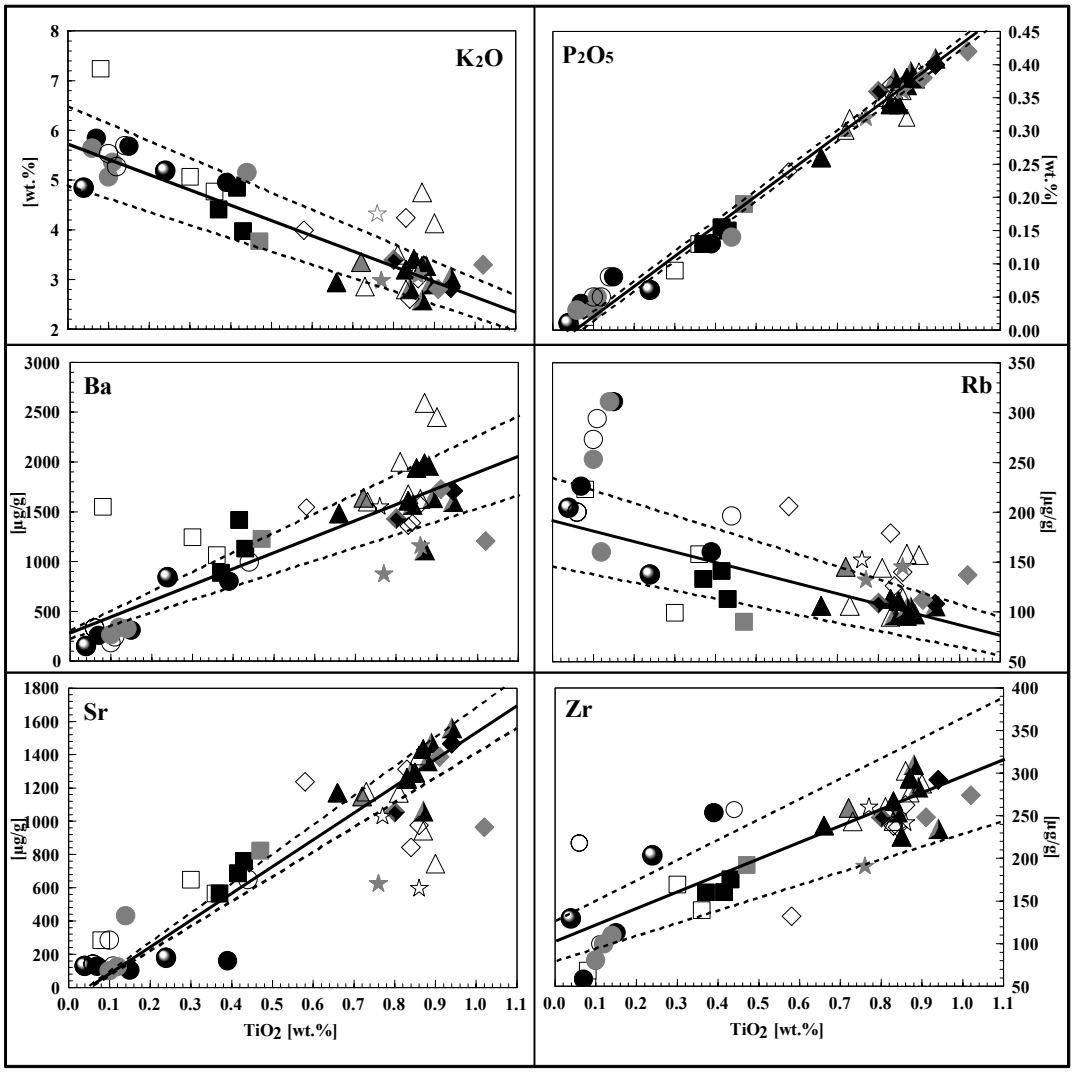

Fig. 1: continued

Within the group of altered Fine- to Medium-grained Granites a significant deviation is observed for Co. There is a marked depletion in three samples which, however, is compensated by an enrichment in three other samples relative to the unaltered equivalents.

The distribution of REE in Småland Granites and Äspö Diorites is fairly homogeneous (see the chondrite-normalized diagrams in Fig. 3). All altered samples plot well within the magmatically produced variation shown as a gray field. For the Fine- to Medium-grained Granites there are two samples which appear slightly above or below the field of fresh rocks.

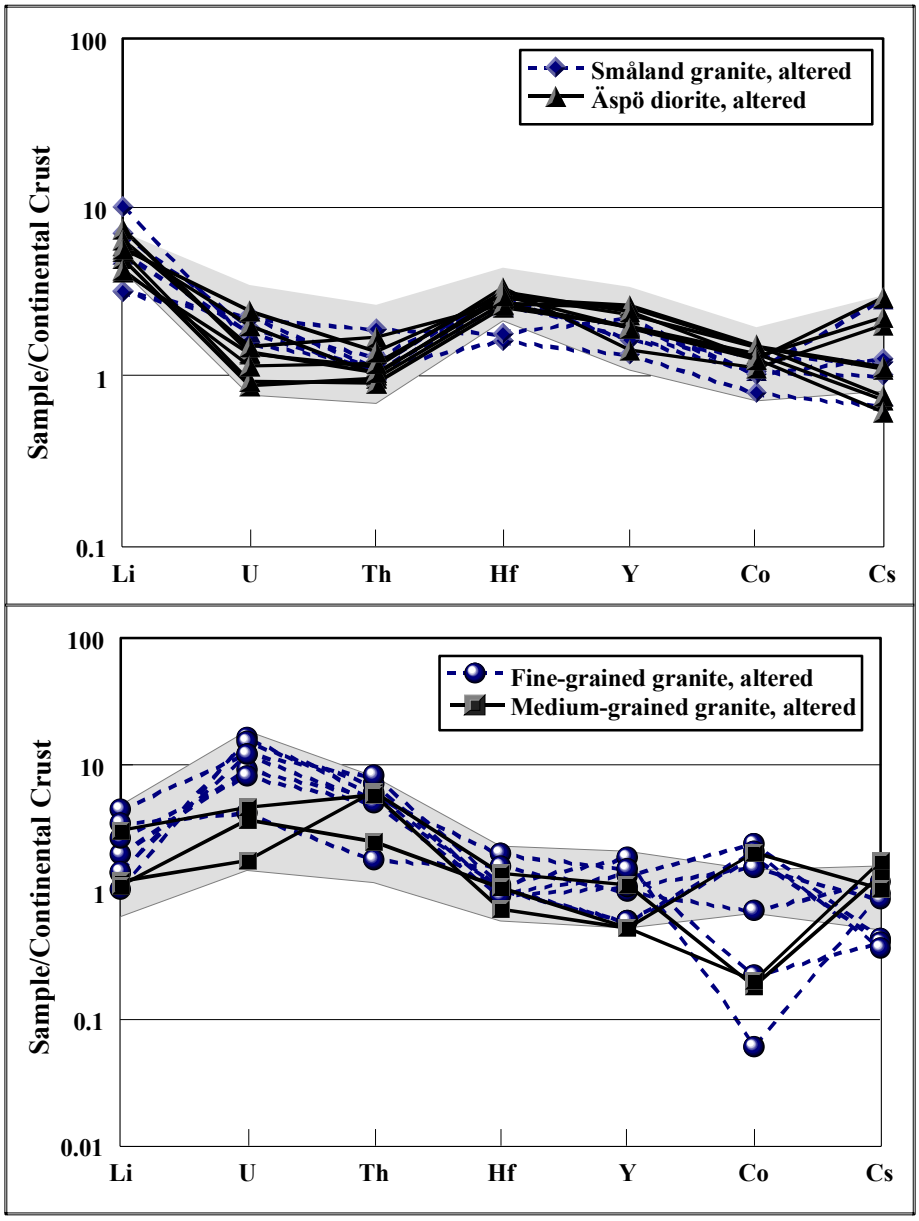

Fig. 2: Distribution of trace elements in altered Äspö granitoids (normalized to whole rock concentration; normalization values according to RUDNICK & FOUNTAIN, 1995; the gray area represents the variation range induced by magmatic processes and analytical errors.

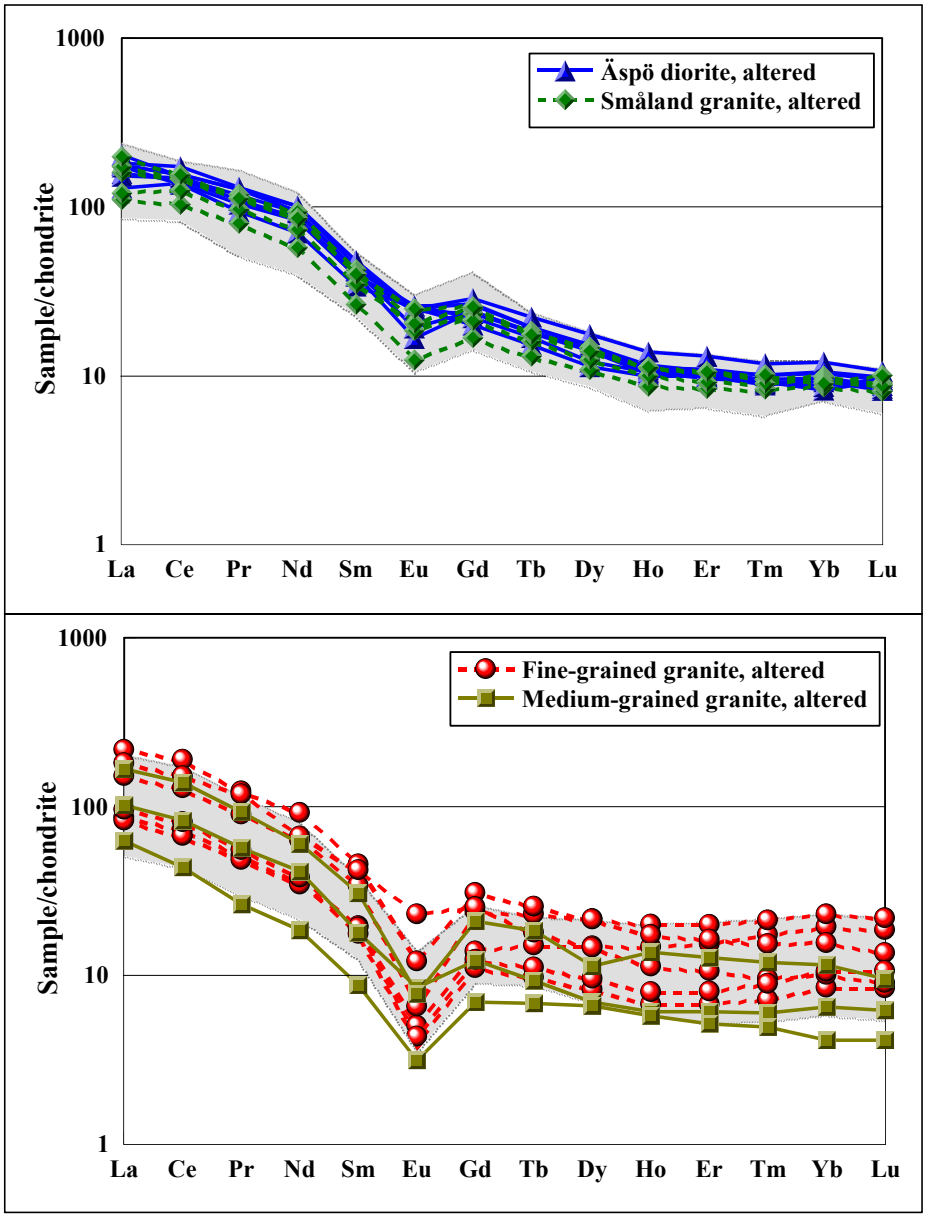

Fig. 3: Distribution of REE in altered Äspö granitoids (normalized to chondritic concentrations; normalization values according to BOYNTON, 1984). The gray fields represent the variation range induced by magmatic processes and analytical errors.

5. Calculation of gain and loss

As outlined in the last paragraph, the hydrothermally induced element variations are determined on the basis of the differences of altered samples relative to the magmatically induced variation range. From these differences the relative gain or loss of an element in an individual rock sample can be calculated. As an example of how the principles of these calculations work the gain and loss for SiO_2 is shown in Fig. 4.

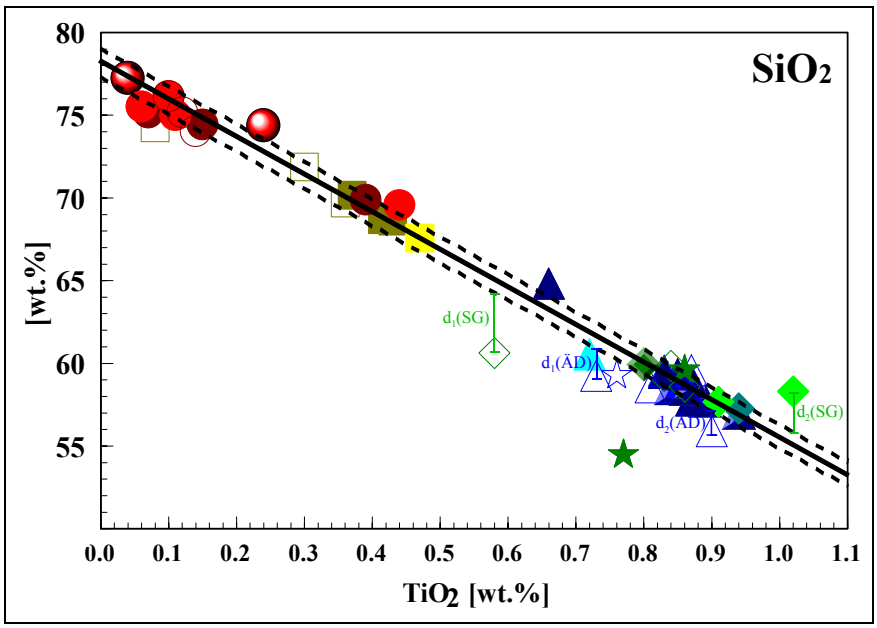

Fig. 4: TiO_2-based diagram for the determination of SiO_2-variations induced by hydrothermal alteration. The solid line represents a linear regression of the fresh Äspö granitoids (stage I), the dashed lines include the natural variation including analytical uncertainties (1σ).

Hydrothermal alteration products are characterized by data points plotting outside the range of variations caused by magmatic processes including the analytical error (1σ). The distance d of an individual data point from the lower or upper limit (dashed lines in Fig. 4) represents the absolute amount of gain or loss at a given TiO_2-value. The sum of all distances - positive or negative - then accumulates to total absolute gain or loss for one rock type, e.g. Småland Granite or Äspö Diorite following the equation:

$$\text{gain/loss [wt.-\%, ppm]} = (\Sigma\, d)N$$

where d is the distance from the linear regression line and N is the number of samples.

Fig. 4 reveals that two data points for altered Äspö Diorites and two for altered Småland Granites plot outside the primary magmatic range represented by the dashed lines. Application of the above equation with positive and negative values for d results in a total loss of 0.57 wt.-% SiO_2 for Småland Granites and Äspö Diorites. The gain and loss of all other elements

plotted in TiO_2-based diagrams was calculated in the same way; the results are presented in Tab. 4. The gain and loss of trace elements which do not refer to TiO_2 are deduced from their deviations from the magmatic ranges plotted in normalized diagrams (Fig. 2 and 3).

Within the set of elements investigated here, some occur outside the range of magmatic variations (including the analytical uncertainty 1 σ). These hydrothermally induced gains and losses are significant for Si, Al, Fe, Ca, K, Ba, Sr, Rb, Li, Cs, Ce, Nd, Sm, Eu and Gd. All the other elements are within the magmatic range.

In the list of elements investigated here, there is a number of chemical components which do not occur as radionuclides in spent fuel. When restricted to repository-related elements, the data presented in Tab. 4 reveal a significant enrichment of Fe, Co, Ba, Ce, Nd, Sm, Eu, and Gd in the altered rocks. Both Äspö Diorites and Småland Granites as well as Fine- and Medium-grained Granites have lost Cs. For Sr, a significant loss is observed in Äspö Diorites and Småland Granites, and Fine- to Medium-grained Granites have obviously gained some Sr. Since the volume abundance of the former rock types is much higher in the Äspö region than that of the latter, a net loss is expected for the behavior of Sr.

This example of gains and losses of elements within a complex assemblage of granitoids as the one found in the Äspö region has demonstrated that principal mechanisms of mobilization and immobilization can be applied to other granites. However, as shown for the case of Sr, there might be specific differences within a given rock volume of granitoids. If, for example, a rock segment is selected for a deep repository which exclusively consists of rock types similar to Fine- and Medium-grained Granites, the behavior of Sr would be different when compared to the Äspö Diorite/Småland Granite-dominated association.

Tab. 4: Relative gain and loss observed in the group of Äspö diorites and Småland granites and in the group of Fine- to Medium-grained granites; significant values for repository-related elements are printed bold.

	Äspö Diorites and Småland Granites		Fine- and Medium-grained Granites	
Element	gain/loss	unit	gain/loss	unit
SiO_2	- 0.57 (± 0.15)	wt. %	- 0.18 (± 0.19)	wt. %
Al_2O_3	- 0.05 (± 0.04)	wt. %	0.00)	wt. %
$Fe_2O_3^{total}$	**+ 0.05 (± 0.04)**	wt. %	**+ 0.02 (± 0.01)**	wt. %
MnO	0.00	wt. %	0.00	wt. %
MgO	+ 0.01 (± 0.04)	wt. %	- 0.02 (± 0.01)	wt. %
CaO	- 0.24 (± 0.02)	wt. %	- 0.26 (± 0.01)	wt. %
Na_2O	- 0.02 (± 0.05)	wt. %	+ 0.01 (± 0.04)	wt. %
K_2O	+ 0.21 (± 0.04)	wt. %	+ 0.14 (± 0.04)	wt. %
Ba	**+ 55.0 (± 32.38)**	ppm	**- 12.3 (± 12)**	ppm
Sr	**- 117 (± 13.22)**	ppm	**+ 131 (± 4)**	ppm
Rb	+ 31.67 (± 4.15)	ppm	- 1.13 (± 0.2)	ppm
Li	+ 0.48 (± 0.09)	ppm	0.00	ppm
Co	0.00	ppm	**+ 1.1 (± 0.5)**	ppm
Y	0.00	ppm	0.00	ppm
Cs	**- 0.05 (± 0.03)**	ppm	**- 0.06 (± 0.02)**	ppm
Th	0.00	ppm	+ 0.10 (± 0.1)	ppm
U	0.00	ppm	0.00	ppm
La	0.00	ppm	0.00	ppm
Ce	0.00	ppm	**+ 1.31 (± 0.8)**	ppm
Pr	0.00	ppm	+ 0.09 (± 0.09)	ppm
Nd	0.00	ppm	**+ 0.49 (± 0.3)**	ppm
Sm	0.00	ppm	+ 0.14 (± 0.08)	ppm
Eu	0.00	ppm	**+ 0.06 (± 0.01)**	ppm
Gd	0.00	ppm	+ 0.07 (± 0.05)	ppm
Tb	- 0.02 (±0.01)	ppm	+ 0.01 (± 0.01)	ppm
Dy	0.00	ppm	+ 0.11 (± 0.1)	ppm
Ho	+ 0.01 (± 0.01)	ppm	- 0.10 (± 0.1)	ppm
Er	0.00	ppm	0.00	ppm
Tm	0.00	ppm	0.00	ppm
Yb	0.00	ppm	- 0.01 (± 0.01)	ppm
Lu	0.00	ppm	+ 0.01 (± 0.01)	ppm

6. Determination of epidote retention capacity

6.1 Epidote-fluid reactions

In contrast to naturally occurring mobilization and immobilization, the experimental approach envisages a worst case scenario where the technical barrier has failed, radionuclide-bearing solutions are released from canisters into the geological barrier and then react with the constituent minerals of the granitoids. The scenario further assumes that the rock mass in direct contact with the technical barrier is locally heated to temperatures of about 50 - 100^{o}C.

From a crystal chemistry point of view, epidote is the only mineral present in Äspö Diorites and Småland Granites which is capable of incorporating significant amounts of U, Th, Y and REE. This mineral forms a continuous line of solid-solution series to the mineral allanite. The distribution of octahedral and tetrahedral sites in the epidote lattice is shown in Fig. 5.

Before the exchange reactions between epidote and trace element enriched solutions are discussed in detail, it is useful to compare some crystal chemical aspects of the epidote-allanite system which are necessary to understand the uptake of large-ion elements from hydrothermal solutions. The general formula of epidote and allanite is best written as

$$\mathbf{A_2\,M_3\,[(SiO_4\,Si_2O_7\,O/OH,F)]},$$

where for epidote the A-position is usually occupied by Ca and the M position by Al and Fe^{3+}. In allanite, these positions are occupied by Ca, Sr, Pb, Mn, REE, Th and U on the A-site (nine- to ten-fold coordinated) and Al, Fe^{2+} and Mg on the octahedral M-site (six-fold coordinated). The reaction from epidote to allanite involving a hydrothermal fluid requires the exchange of ferric iron in epidote with ferrous iron in allanite in order to maintain charge balance if trivalent REE are incorporated.

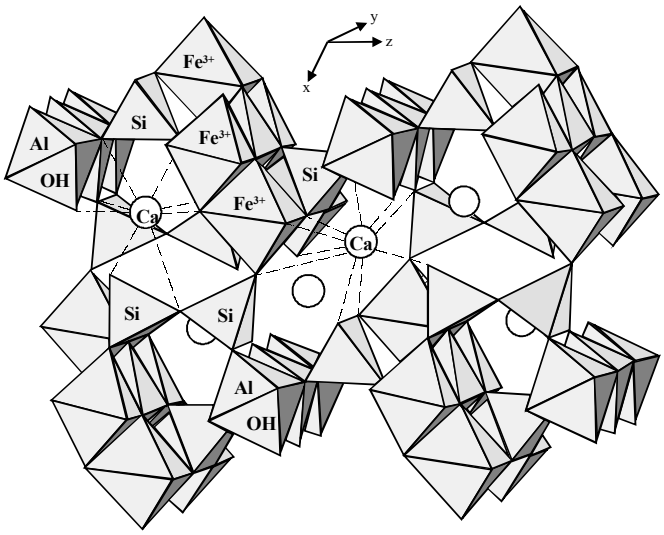

Fig. 5: Three-dimensional plot showing coordination polyhedra of the epidote lattice (after Deer et al., 1998): tetrahedral sites are occupied by Si and Al, octahedral sites contain Al, Fe^{2+}, Fe^{3+}, Mn, Mg etc.; Ca is nine- or ten-fold coordinated; x-y-z refers to crystallographic orientation.

Because of its structural and crystal chemical state, epidote can take up some repository-related elements in significant quantities. As trans-uranium elements cannot be handled in conventional experimental setups, the REE have been used as analogues, e.g. Ce as Ce^{4+} has an effective ionic radius of 104 pm and is thus geochemically similar to Np, Pu and Am, which have effective ionic radii of 98 to 105 pm (ionic radii data from Shannon, 1976).

Experiments have been conducted as outlined in the Appendix Chapter A4. Before exchange reactions for the determination of partition coefficients could be tested, it was necessary to check for any time-dependence on exchange rates. Therefore, a set of experiments was carried out in which the effects of run duration were investigated and found to be negligible for run durations of more than 3 days (results summarized in Johannes, 2000).

Tab. 5 shows that at temperatures of 450 and 550°C, 80 to 90 % of the original fluid contents are located in the bulk solid. At 250°C, only Ce, Th and U are incorporated in the solid in appreciable amounts. The concentrations of the other elements decrease continuously with decreasing temperatures. Obviously, Ce, Th and U behave alike as a group when compared to La, Nd, Eu, Yb, and Y, suggesting that these groups of elements should be discussed separately for further interpretation and for the determination of *D*-values.

Tab. 5: Concentrations analyzed in solid experimental run products at different temperatures. The individual concentrations in the fluids were 10000 ppm Y, La, Ce, Nd, Eu, Yb, Y, and 1000 ppm U and Th.

Experiment Nr.	KEN-37	KEN-38	KEN-40	KEN-45
Temp. [°C]	550	450	350	250
Y	8567	6472	5077	611
La	8811	7631	3575	270
Ce	9154	8998	9147	9069
Nd	9216	7635	4739	343
Eu	8074	6303	4214	444
Yb	8620	8620	8391	2434
Th	998	998	997	997
U	851	687	486	565

Fig. 6 shows details of a typical solid run product obtained at 550°C. Grains of newly formed allanite can clearly be distinguished from those of primary epidote grains, which implies that only parts of the original epidote material has reacted with the fluid.

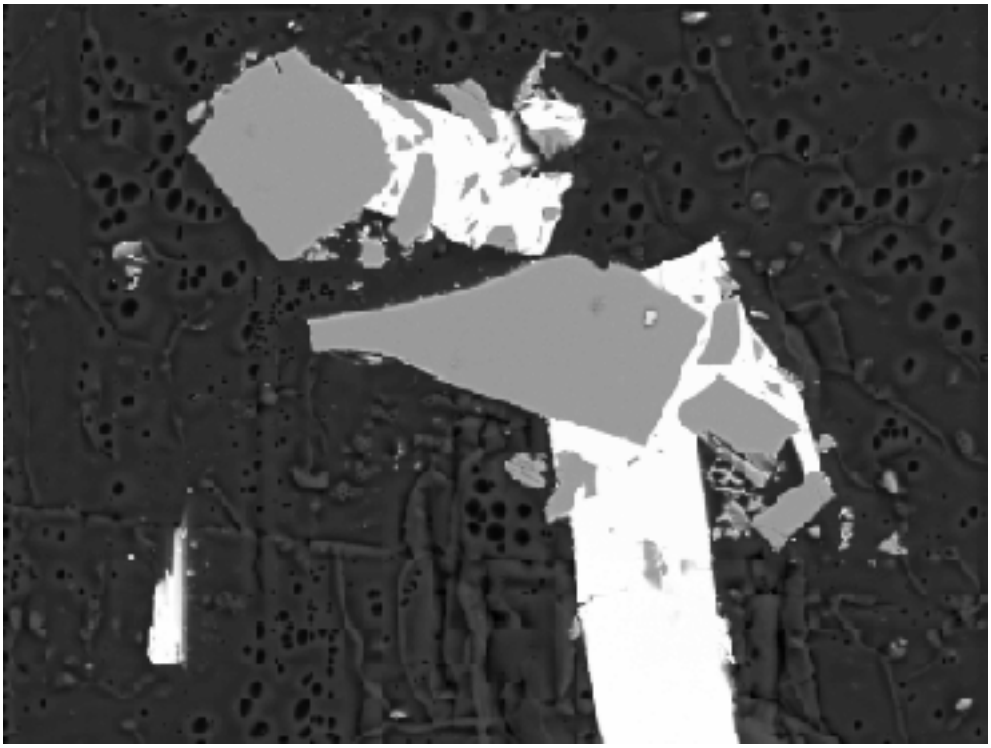

Fig. 6: Back-scattered electron image of an experimental run product showing newly formed allanite (light contours) and unreacted epidote (dark contours), the horizontal image size is 200 µm).

This experimental result was to be expected because the mass of elements introduced by the fluid is too small to allow complete reaction with the solid material to form allanite as the only solid run product. For example, the concentration of Ce in the fluids was 10 000 ppm, which equals a mass of 500 µg Ce in a total of 50 µl fluid used in this experiment. Allanite, however, contains up to 10 wt.-% Ce. If the bulk mass of epidote used (50 mg) was to react to allanite, a total of 5 mg Ce would be necessary. Since only some ten percent of this mass was actually available, only part of the original epidote material could form allanite by uptake of Ce, Th, and U. As a qualitative result of the observation presented in Fig. 6 it is concluded that a large proportion of Ce, Th and U will be removed from a migrating fluid as long as there is enough epidote present that allows the formation of allanite.

6.2 Determination of D-values

In order to study the incorporation of repository-related elements in the epidote-allanite system, temperatures higher than those expected in the near-field of emplaced canisters have to be used because otherwise the experimental times would be intolerably long (probably several decades). It is common practice in experimental petrology to extrapolate results of high-temperature experiments to lower temperatures given the complete miscibility of the mineralogical end-members. The incorporation of repository-related elements can best be described by the mineral/fluid phase distribution coefficient *D,* which is simply derived by dividing the concentrations measured in the solid by the concentration measured in the coexisting fluid. In all natural systems, the value of *D* depends on temperature, pressure and the bulk chemistry of the system. As the bulk chemical system is defined by the epidote-allanite mineral group and the pressure is kept constant at 50 MPa, it is only the temperature dependence on *D* which has to be accounted for. Thus, experiments have been designed for epidote-fluid reactions in the temperature range of 550 to 250°C, a range which is broad enough to allow extrapolation of the *D*-values down to 100 and 50°C.

A full description of all experimental details and individual analyses of run products is given by Johannes (2000). Here, the key results of four representative experiments at 550, 450, 350, and 250°C are reported which are used for the calculation and extrapolation of *D*-values to 100 and 50°C (see also Appendix Tab. A5). There is a strong temperature dependence for incorporation of La, Nd, Eu, Yb and Y, whereas the respective temperature dependence is less pronounced for Ce, Th and U. The uncertainties for the analytical measurements are ± 5 % for both the solid run products and the coexisting liquids. From the data given in Tab. A5, the partition coefficients *D* are derived by dividing the value obtained for the trace element contents in the solid by that of the coexisting liquid. The resulting *D*-values and their extrapolation to 100 and 50°C are given in Tab. 6.

Tab. 6: Partition coefficients for epidote/allanite and hydrothermal fluid at temperatures ranging from 550 to 250°C and extrapolation to T=100°C and T=50°C. Note that for Y, La, Nd, Eu and Yb, *D*-values are below 1 at temperatures ≤ 250°C.

Run Nr.	KEN-37	KEN-38	KEN-40	KEN-45	*D*	*D*
T (°C)	550	450	350	250	*100*	*50*
Y	168	3.0	1.4	0.1	*≤ 0.02*	*≤ 0.02*
La	190	6.2	0.7	0.03	*≤ 0.02*	*≤ 0.02*
Nd	181	4.7	1.0	0.04	*≤ 0.02*	*≤ 0.02*
Eu	141	3.4	1.1	0.1	*≤ 0.02*	*≤ 0.02*
Yb	304	300	33	0.4	*≤ 0.02*	*≤ 0.02*
Ce	**852**	**541**	**205**	**95**	***50***	***30***
Th	**9975**	**9400**	**4456**	**5616**	***1512***	***1100***
U	**4221**	**4.2**	**4.2**	**8.9**	***10***	***8***

Due to the analytical error of ± 5 % mentioned above, error propagation for the *D*-values results in total uncertainties of ± 7.1 % (rel.). Fig. 7 shows a clearly different behavior of Ce, Th and U relative to La, Nd, Eu, Yb, and Y. The latter group of elements reveals incorporation

in epidote/allanite with D >1 only at temperatures above 350°C above, and has D < 1 at temperatures below 250°C. In contrast, Ce, Th, and U have D-values unity at all experimental temperatures with a temperature dependence more pronounced for Ce than for Th.

Summarizing the results for experimentally determined partitioning between epidote and trace element-enriched hydrous fluids it must be emphasized that at repository-relevant temperatures near 50 to 100°C, only Ce, Th and U are significantly taken up in the epidote structure. The respective partition coefficients are plotted bold in Tab. 6. In contrast to Ce, Th, and U, all other elements investigated show a behavior incompatible with epidote at 50 to 100°C. As a consequence, the potential retention capacity of epidote in the geological barrier can only be calculated for U and Th and for actinides that behave geochemically similar to U and Ce, i.e. Pu, Np, and Am.

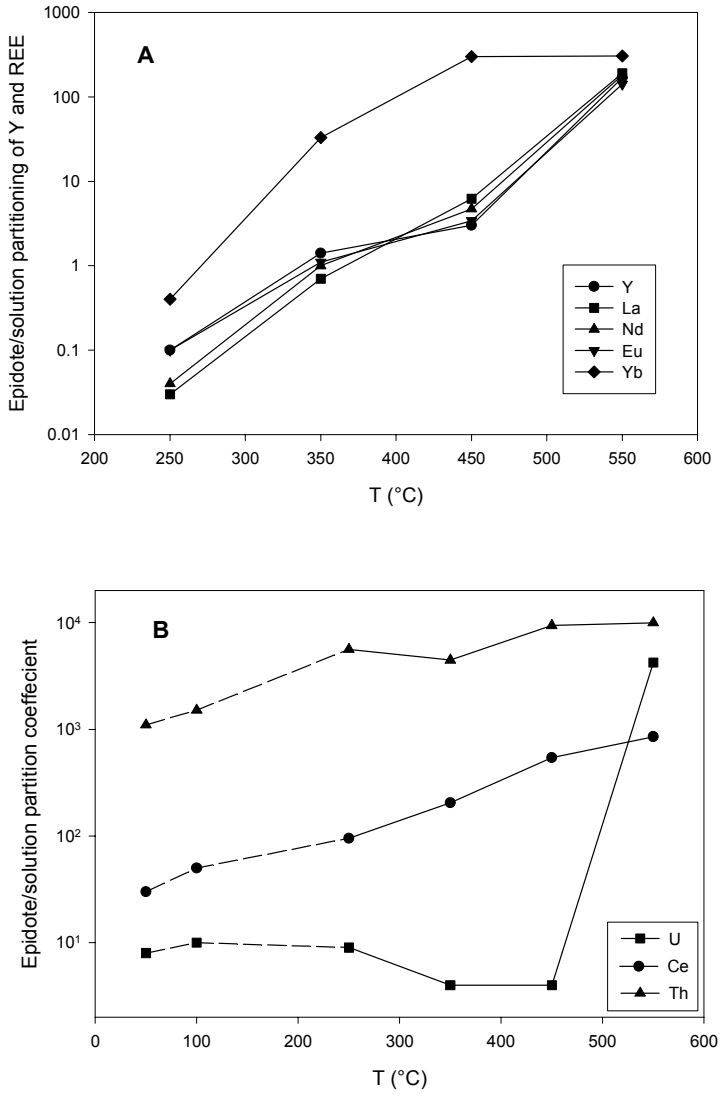

Fig. 7: Partition coefficients *D* for the distribution of trace elements as a function of temperature. Experimentally derived *D*-values are plotted as closed symbols, extrapolated *D*-values are shown as open symbols. For the elements shown in A (Y, La, Nd, Eu, Yb) *D*-values are < 1 at temperatures ≤ 250°C. Ce, Th, and U have high *D*-values including the extrapolated

temperature range of T=250°C to T= 50°C (dashed lines).

7. Retention capacity of the geological barrier granite

The immobilization capability of repository-related elements in granitic rocks from Äspö is evaluated in a combined approach which is based on the retention capacity of hydrothermally altered granitic rocks and on the specific retention capacity of the mineral epidote contained in them. Calculating the retention capacity of granites requires additional information on

1) the rock volume heated to temperatures between 50 and 100°C,
2) the mass of water which is available to transport radionuclides from canisters through the rock matrix, and
3) the radionuclide inventory and the total mass of spent fuel expected to be deposited.

7.1 Volume of heated rock (matrix volume)

Recent SKB publications on post-closure safety (SKB 1999) include three models described for the scenarios *Aberg*, *Beberg*, and *Ceberg*. The model presented here is based on the *Aberg* scenario and on the calculations for heat transfer and heat distribution in the rock matrix as reported in SKB (1999, Chapter 8.6) and by Janson and Koukkanen (1999). If we assume the following conditions, based on SKB (1999), the volume of granite matrix heated to temperatures of 50°C by transport of heat from buried canisters can be calculated:

- The number of canisters is 4000, deposited at 600 m depth within 10 years.
- The maximum temperature at the outer metal surface does not exceed 100°C; the distance between individual containers is 6 m each and allows a temperature of up to 50°C in the rock matrix.
- Canisters are deposited on two superimposed levels; the vertical distance between the upper and the lower tunnel is 50 m.
- the height of the heated rock matrix around the two superimposed tunnels is 140 m.

On the basis of these assumptions, the volume of the rock matrix heated to 50°C is $5 \cdot 10^7$ m^3.

7.2 Mass of underground water within the matrix volume

The mass of radionuclides transported from leaking canisters through the rock matrix crucially depends on the mass of water flowing through a given volume of granite in a given period of time. The following assumptions are made to calculate the time-integrated water/rock ratio.

- The repository is located in undisturbed rock masses, i.e. fractures and fracture zones of high water conductivity are avoided.
- Average flux of underground water flux is 3 liters m^{-2} a^{-1}.
- Migrating water is heated to rock temperature (50°C) and moves pervasively through the

rock mass.

- All canisters leak simultaneously and migrating underground solutions have access to the radionuclide inventory.

Usually the water/rock ratios of interactions of granites with hydrothermal solutions are derived from oxygen and hydrogen isotope fractionation. Simon (1990) reports a water/rock ratio of 0.9 for the Black Forest Granites (SW Germany). Application of the groundwater flux suggested by SKB (1999) of 3 liters m^{-2} a^{-1} for the *Aberg* groundwater flux models results in $1.3 \cdot 10^7$t water running through $5 \cdot 10^7$ m^3 of granite within 10000 a. At a rock density of 2.8 t/m^3 the water/rock ratio is 0.09. This value is almost ten times lower than that expected for the natural alteration of granites. It seems reasonable to apply this low water/rock ratio of 0.09 to the radionuclide transport discussed here, because the time scale of natural processes, as exemplified for the Black Forest Granites, is at least two orders of magnitude larger than that expected for artificially heated granite. Nevertheless, the consequences of a water/rock ratio of 0.9 ($1.3 \cdot 10^8$ t water) will also be considered here in order to cover conservative assumptions.

7.3 Inventory of radionuclides in an underground repository

According to the data base given by SKB (1999), the mass of repository-related elements can be calculated by adding up individual nuclides. The radionuclide inventory compiled by SKB (1999, TR 96-06: Table 6-1) includes the activities of 80 individual nuclides (fission products, actinides and actinide daughters, activation products) 40 years after discharge from the reactor. The inventory of the repository-related elements analyzed here is summarized in Tab. 7 (nuclides of elements not studied here not considered). The right column in Tab. 7 contains the accumulated mass of nuclides in 8000 tons of spent fuel.

Tab. 7: Calculation of the radionuclide inventory of Fe, Co, Sr, Y, Cs, Ba, REE, Th, U, Np, Pu, and Am, contained in average spent fuel 40 years after discharge. Source of data: Column 2: Karlsruher Nuklidkarte, column 3: SKB 1999. Subscripts $_{(A)}$, $_{(F)}$ and $_{(A+AD)}$ denote activation product, fission product, and actinide plus actinide daughter, respectively. The bold-type figures in column 5 represent the masses of elements accumulated from the respective nuclides of each element.

Nuclide	λ (a^{-1})	Activity (decays/a·t) in 8000 t spent fuel	Mass of nuclide in 8000 t spent fuel	Mass of element in 8000 t spent fuel
$^{55}Fe_{(A)}$	0.2539	$9.30 \cdot 10^{9}$	$8.44 \cdot 10^{-7}$ t	**<0.0001 t Fe**
$^{60}Co_{(A)}$	0.1315	$8.90 \cdot 10^{11}$	0.000170 t	**0.0002 t Co**
$^{90}Sr_{(F)}$	0.0240	$1.20 \cdot 10^{15}$	1.87 t	**1.88 t Sr**
$^{90}Y_{(F)}$	94.7	$1.2 \cdot 10^{15}$	0.00047 t	**0.0005 t Y**
$^{135}Cs_{(F)}$	$3.01 \cdot 10^{-7}$	$2.1 \cdot 10^{10}$	3.94 t	**8.42 t Cs**
$^{137}Cs_{(F)}$	0.023	$1.8 \cdot 10^{15}$	4.48 t	
$^{137}Ba_{(F)}$	142757	$1.7 \cdot 10^{15}$	$6.83 \cdot 10^{-7}$ t	**<0.0001 t Ba**
$^{147}Pm_{(F)}$	0.264	$1.5 \cdot 10^{11}$	$3.49 \cdot 10^{-5}$ t	**<0.0001 t Pm**
$^{151}Sm_{(F)}$	0.0077	$9.4 \cdot 10^{12}$	0.0772 t	**0.0772 t Sm**
$^{154}Eu_{(F)}$	0.0806	$1.80 \cdot 10^{13}$	0.0143 t	**0.0150 t Eu**
$^{154}Eu_{(A)}$	0.0806	$3.20 \cdot 10^{11}$	0.000255 t	
$^{155}Eu_{(F)}$	0.1455	$7.60 \cdot 10^{11}$	0.000338 t	
$^{230}Th_{(A+AD)}$	$9.19 \cdot 10^{-6}$	$1.60 \cdot 10^{7}$	0.000171 t	**0.0002 t Th**
$^{234}U_{(A+AD)}$	$2.82 \cdot 10^{-6}$	$4.60 \cdot 10^{10}$	1.60 t	**7793 t U**
$^{235}U_{(A+AD)}$	$9.84 \cdot 10^{-10}$	$4.50 \cdot 10^{8}$	45.0 t	
$^{236}U_{(A+AD)}$	$2.96 \cdot 10^{-8}$	$1.00 \cdot 10^{10}$	33.4 t	
$^{238}U_{(A+AD)}$	$1.55 \cdot 10^{-10}$	$1.20 \cdot 10^{10}$	7713 t	
$^{237}Np_{(A+AD)}$	$3.23 \cdot 10^{-7}$	$1.50 \cdot 10^{10}$	4.60 t	**4.60 t Np**
$^{238}Pu_{(A+AD)}$	0.00790	$9.50 \cdot 10^{13}$	1.20 t	**52.8 t Pu**
$^{239}Pu_{(A+AD)}$	$2.87 \cdot 10^{-5}$	$9.50 \cdot 10^{12}$	33.1 t	
$^{240}Pu_{(A+AD)}$	$1.05 \cdot 10^{-4}$	$1.20 \cdot 10^{13}$	11.4 t	
$^{241}Pu_{(A+AD)}$	0.0483	$7.70 \cdot 10^{14}$	1.61 t	
$^{242}Pu_{(A+AD)}$	$1.86 \cdot 10^{-6}$	$1.00 \cdot 10^{11}$	5.46 t	
$^{241}Am_{(A+AD)}$	0.00160	$1.50 \cdot 10^{14}$	9.44 t	**10.8 t Am**
$^{242}Am_{(A+AD)}$	0.00491	$4.50 \cdot 10^{11}$	0.00928 t	
$^{243}Am_{(A+AD)}$	$9.40 \cdot 10^{-5}$	$1.20 \cdot 10^{12}$	1.30 t	

7.4 Retention capacity of altered granites

The essential parameter for calculating the retention capacity of the granite matrix is the gain or loss which describes the absolute extent to which an individual element is immobilized with respect to migrating hydrous solutions or is leaked from the rock matrix. The gains and losses for the repository-related elements analyzed here have been summarized in Tab. 4 for a model volume of 1 km^3 of Äspö granitoids. These data are used here to calculate the retention capacity of an individual element *i* in a smaller matrix volume (*MV*, $5 \cdot 10^7$ m^3) of $1.4 \cdot 10^8$ t

Äspö granitoids (ρ=2.8 g/cm^3) by the equation

$$RC^i = (x \cdot GL^i_A + y \cdot GL^i_B + z \cdot GL^i_C) \cdot MV \cdot \rho$$

where *x, y, z* are the relative abundances of altered Äspö Diorites, Småland Granites and Fine- to Medium-grained Granites, respectively, and $GL_{A,B,C}$ are the gains and losses of element *i*. The calculated retention capacities for the heated rock mass (matrix volume) of $5 \cdot 10^7$ m^3 Äspö granitoids are summarized in Tab. 8.

Tab. 8: Retention capacity of repository-related elements (actinides not considered) in an assumed matrix volume of $5 \cdot 10^7$ m^3 Äspö granitoids

	Total mass of elements in 8000 t spent fuel (t)	Retention capacity of a model repository volume $5 \cdot 10^7$ m^3	Percentage of nuclides which can be immobilized
Fe	<0.0001	46060 t	100 %
Co	0.0002	15 t	100 %
Y	0.0005	0 t	none
Sr	1.88	0 t	none
Cs	8.42	0 t	none
Ba	<0.0001	6756 t	100 %
Pm	<0.0001	(Nd) 7 t	100 %
Sm	0.0772	2.0 t	100 %
Eu	0.015	0.8 t	100 %

The retention capacity of Fe, Ba, Co, Pm, (Nd), Sm, and Eu is much higher than the amount contained in 8000 t of spent fuel, which implies that the respective nuclides could all be retained in the granite matrix. The retention capacity of the highly mobile elements Cs and Sr is zero and so is the retention capacity of the rather immobile element Y. For U and Th no retention capacities could be calculated because of the very low variability of these elements in the Äspö granitoids. The same applies to other actinides, because nuclides with masses > 238 do not occur in natural rocks. Their retention capacity can be better understood in terms of their potential uptake in epidote.

7.5 Retention in epidote/allanite

The presence of the mineral epidote in altered granitoids will certainly result in a strong immobilization of actinides from underground solutions at elevated temperatures, because the partition coefficients for these elements between solution and epidote are well above unity at 50 to 100°C (see Tab. 6).

In order to calculate the effect of epidote on the retention capacity of actinides the following assumptions are necessary:

a) Ce is an adequate natural analogue for Np, Pu, and Am,

b) the availability of underground water is sufficient to dissolve and transport radionuclides,

c) epidote has a small grain size and is homogeneously distributed in the reference volume,

d) the prevailing temperature in the barrier (matrix volume, $5 \cdot 10^7$ km^3) is 50 to100^{o}C.

The maximum concentration of U in natural aqueous solutions under mildly reducing conditions is $7 \cdot 10^{-5}$ Mol U/l in the central pH range of 5 to 8 (Gascoyne 1988). This concentration equals 16.6 µg/g. Tab. 9 summarizes the maximum solubility for other relevant actinides, *D*-values and the resulting retention capacities for epidote in the matrix volume.

The calculations are based on the equation

$$RC^i_{epidote} = c^i_{sol} \cdot K^i_D \cdot x_{epidote} \cdot MV \cdot \sigma_{MV},$$

where for an element *i* the retention capacity of epidote $RC_{epidote}$ is defined as the product of the concentration in the migrating underground solution c_{sol}, the partition coefficient *D,* the fraction of epidote $x_{epidote}$ present in Äspö granitoids, the mass of the assumed matrix volume *MV,* and the density of Äspö granitoids ρ (2.8 g/cm^3). It should again be emphasized that unlike the *D* values widely used in near-field and far-field scenarios, the partition coefficient used here has no dimension and refers to the chemical equilibrium constant for the exchange of an element between a solid and a fluid phase, i.e. $D=c_{solid}/c_{fluid}$.

Tab. 9: Solubility and mass of dissolved elements in $1.3 \cdot 10^7$ and $1.3 \cdot 10^8$ t of water (water/rock ratios of 0.09 and 0.9, respectively) and percentage of radionuclides dissolved from 8000 t of spent fuel.

	Solubility in under-ground water (t/t)	Mass in 8000 t spent fuel (t)	Mass of element dissoluble in $1.3 \cdot 10^7$ t water	Mass of element dissoluble in $1.3 \cdot 10^8$ t water	Fraction of element dissolved relative to bulk spent fuel in $1.3 \cdot 10^7$ t	Fraction of element dissolved relative to bulk spent fuel in $1.3 \cdot 10^8$ t
Th	$4.7 \cdot 10^{-10}$	0.0002	0.006	0.060	100%	100%
U	$1.7 \cdot 10^{-5}$	7793	217	2170	2.8%	28%
Np	$4.7 \cdot 10^{-8}$	4.6	0.61	6.1	13%	100%
Pu	$7.3 \cdot 10^{-7}$	52.8	9.5	95	18%	100%
Am	$1.7 \cdot 10^{-6}$	10.8	22.1	221	100%	100%

Tab. 9 shows that only a small fraction of the bulk mass of uranium is dissolved at either water/rock ratio. The same applies to Np and Pu, which to a large extent are not dissolved by migrating underground solutions at a water/rock ratio of 0.09. If, however, a water/rock ratio of 0.9 is assumed ($1.3 \cdot 10^8$ t water), all actinides will enter the migrating underground solution with the exception of U, which is dissolved to a degree of 28 %.

The amount of actinides being immobilized by epidote depends on the concentration of actinides in solution, on the mass of water and the mass of epidote available. Although the partition coefficients for actinides between epidote and water are high, a certain fraction of actinides could still remain in the solution after chemical equilibrium between fluid and epidote has been achieved. Tab. 10 summarizes the amount of actinides being fixed in epidote and the amount still being in solution considering water/rock ratios of 0.09 ($1.3 \cdot 10^7$ t water,

case A) and 0.9 ($1.3 \cdot 10^8$ t water, case B).

Tab. 10: Masses of actinides immobilized at different water/rock ratios. Case A: Water/rock ratio = 0.09, i.e. $1.3 \cdot 10^7$ t of water in $1.4 \cdot 10^8$ matrix volume. Case B: water/rock ratio=0.9, i.e. $1.3 \cdot 10^8$ t of water in $1.4 \cdot 10^7$ matrix volume.

	Mass dissolved Case A (t)	Tons dissolved Case B (t)	*D*	Mass fixed in epidote		Mass remaining in undergr. solution		Fraction immobilized	
				Case A (t)	Case B (t)	Case A (t)	Case B (t)	Case A %	Case B %
Th	0.0002 t	0.002 t	1100	0.0055 t	0.0055 t	$< 10^{-6}$	$< 10^{-6}$	100 %	100 %
U	204 t	2040 t	8	204 t	1123 t	0.1	917	99.9 %	55 %
Np	0.58 t	4.6 t	30	4.6 t	4.4 t	$< 10^{-6}$	0.23	100 %	95 %
Pu	9.0 t	50.3 t	30	50 t	48 t	$< 10^{-6}$	2.52	100 %	95 %
Am	9.3 t	9.3 t	30	9.3t	8.8 t	$< 10^{-6}$	0.45	100 %	95 %

Tab. 10 clearly shows that the amount of epidote present in the matrix volume of $5.\cdot 10^7$ m^3 rock mass is capable of retaining nearly 100 % of the dissolved actinides (U: 99.7%) in the realistic case A ($1.3 \cdot 10^7$ t water, water/rock ratio=0.09). At a ten times higher water/rock ratio (case B), only Th is completely immobilized from the solution, and 95 % of Np, Pu, and Am are immobilized and the amount of U fixed in epidote is just 55 % of the total U dissolved in $1.3 \cdot 10^8$ t underground water.

A water/rock ratio of 0.9 is common in the reaction of granites with hydrothermal solutions (e.g. Simon 1990), but is unlikely to be achieved in the matrix volume of granite discussed here. There are two possible ways to deal with such high water/rock ratios: either the flux of underground water is ten times higher (30 instead of 3 liters $m^{-2} \cdot a^{-1}$), or the residence time for the solutions is increased from 10000 to 100000 a. Both assumptions are regarded to be highly improbable, implying that at realistic water/rock ratios the radionuclides investigated here will be retained completely in epidote of the granite matrix.

7.6 Summary of radionuclide retention of granite

The retention capacity of granite for the repository-related elements investigated here can in summary be taken to result from

- the uptake of trace elements from underground solutions by the alteration of silicate minerals (feldspars, mica) of the granite matrix, and
- the uptake of trace elements from solutions by incorporation into epidote also contained in the granite matrix.

The results obtained in the previous section are summarized in Tab. 11 and are compared to the mass of elements contained in 8000 t of spent fuel, which corresponds to the total amount of nuclear waste to be deposited in Sweden. The upper section of Tab. 11 represents the retention by the granitic matrix volume, the lower section represents the retention calculated for epidote contained in the same volume of Äspö granitoids.

Tab. 11: Retention of repository-related elements in the rock matrix (lines Fe to Eu) and in epidote (lines Th to Am). The data from column B are from Tab. 7 . Column D denotes the fraction of radio nuclides immobilized from the maximum load of contaminated underground solutions.

	A	B	C	D
Element	Retention in the matrix volume (t)	Mass of element present in 8000 t of Swedish spent fuel (t)	Fraction immobilized in granite matrix (%)	Fraction immobilized from contaminated solutions (%)
Fe	46060	<0.0001	100	
Co	15	0.0002	100	
Sr	none	1.9	0	
Y	none	0.0005	0	
Cs	none	8.1	0	
Ba	6756	<0.0001	100	
Pm(Nd)	7	<0.0001	100	
Sm	2	0.077	100	
Eu	0.8	0.015	100	
Th	0.006	0.0002		100
U	204	7793		99.9
Np	4.6	4.6		100
Pu	50	52.8		100
Am	9.3	10.8		100

The elements Sr and Cs, which are highly mobile in aqueous solutions, are not fixed by altered granites at all. The same applies to Y. On the basis of the results obtained here it is concluded that the total inventory of radionuclides of Fe, Co Ba, Pm, Sm, and Eu may be immobilized

completely in the geological barrier. Given the small solubility of actinides in a realistic volume of underground solutions, the maximum load contained in a contaminated solution will also be immobilized completely by uptake in epidote.

It is concluded that granitic rocks do have a significant immobilization capacity for a number of repository-related elements as long as a deposition volume is selected which is virtually free of high-transitive fractures, contains epidote-bearing altered granitoids and has a geometry similar to that envisaged by SKB (1999), i.e. 6 m distance between individual canisters. The model discussed here assumes a temperature around 50^{o}C prevailing in the rock matrix. Should the heat transfer to the rock matrix result in higher temperatures of the rock matrix, the immobilization capacity of epidote-bearing rocks is also predicted to increase due to the positive slope of epidote *D* values with increasing temperature.

8. Summary and conclusions

The mobilization and immobilization of repository-related elements in granitic rocks can be derived from observations of reactions between migrating hydrothermal underground solutions that have affected the granitoids in the geological past. The observations made here are based on a reference volume of one km^3 of representative granite rocks. For any repository planned in large volumes of altered granites, individual analyses of the gain and loss of repository-related elements are essential. Since the granitoids of the Äspö region are similar to other granite formations in Central Europe regarding their mineralogical and chemical composition, the main results can be expected to be applicable to various other sites in the 'crystalline' underground, too.

The review of chemical retention that has occurred in the geological past is restricted to those elements that are mobile in granites on a cm- to dm-scale. This applies to a large number of elements investigated here: the soluble elements Sr and Cs (and to some extent Y) are not immobilized by sorption to the rock matrix, but Fe, Co, Ba and REE are fixed in secondary minerals formed *in-situ*, i.e. they are fixed immediately by the replacement of primary magmatic minerals. However, the behavior of actinides could not be determined by this approach, because they did not take part in mobilization/immobilization reactions.

The presence of epidote in granitic rocks generally makes a retention capacity of actinides possible because a solid-solution series exists between Ca-Fe epidote and Th-, U-, REE-epidote, the latter being known as allanite. Direct analysis of epidotes contained in granites is not helpful in exploring the retention capacity of REE and actinides, because we simply do not know at which concentration levels these elements have been transported and reacted in migrating solutions being in equilibrium with epidote. Therefore, the chemical partition coefficients between epidote and hydrothermal fluids for these elements were determined under controlled P,T and f_{O2} conditions. Since trans-uranium elements cannot be used in conventional experimental set-ups, the behavior of LREE - and among these of Ce in particular - was investigated. Because of the chemical properties of Ce, it may serve as a natural analogue for Np, Pu and Am. When extrapolated to lower temperatures, partition coefficients well above unity resulted for Th, U, and Ce, which implies that in a temperature range of 50 to 100°C these elements along with Np, Pu, and Am are incorporated into the epidote lattice to a large extent.

The main results obtained from the analysis of a reference volume and from experimental element partitioning can be applied to a model repository located in massive granite where large fracture systems do not have access to rock masses selected for deposition. Whereas the calculation of the retention of Fe, Co, Y, Sr, Cs, Ba, and REE by the granitic matrix is simply derived from the reduction of the results obtained for a one km^3 reference volume, the partitioning of actinides into epidote requires a number of additional assumptions. The model repository discussed here is closely related to the conditions reported for the hypothetical location *Aberg* by SKB. In order to maintain conservative assumptions, a number of conditions were chosen which control the retention of actinides by epidote contained in approximately 5 % of the reference volume. Among these assumptions are: shortly after deposition, the technical barrier fails and migrating underground solutions have access to all 4000 canisters buried at 600 m depth. If the unrealistic values for water/rock ratios of 0.9 are

omitted, the calculations have as a result the complete immobilization of actinides at a realistic water/rock ratio of 0.09, thus preventing them from being part of the fraction incorporated in solution. The only exception is U, about 0.1 percent of which remains in solution and may be transported into the biosphere.

The approach pursued here shows that granitic rocks may serve as a very effective geological barrier for spent fuel deposited at depth. With the exception of highly mobile elements like Sr and Cs, all other repository elements investigated here are completely immobilized by the granite matrix. However, this investigation did not include some of the other highly mobile radionuclides also contained in spent fuel, such as Ag, Sn, and Ra, and gaseous compounds have not been dealt with, either. Thus, the results obtained in this study for naturally occurring elements in granites do not fully account for all aspects of radionuclide mobilization and immobilization but nevertheless offer an important insight into problems of the radionuclide immobilization of spent fuel potentially being deposited in an underground repository of granite formations.

9. References

Beattie, P., Drake, M., Jones, J., Leemann W., Longhi, J., McKay, G., Nielsen, R., Palme, H., Shaw, D., Takahashi, E., and Watson, B. (1993) Terminology for trace element partitioning. Geochim. Cosmochim. Acta 57: 1605-1606.

Boynton, W.V. (1984) Geochemistry of the rare-earth elements: meteorite studies. In: Henderson, P (editor): Rare earth element geochemistry, Elsevier, pp. 63 - 114.

Deer, W.A., Howie, R.A. and Zussman, J. (1998) An introduction to the rock forming minerals. Addison Wesley Longman Limited.

Gascoyne, M. (1992) Geochemistry of the actinides and their daughters. In: Ivanovich, M. and Harmon, R.S. Uranium-series disequilibrium: Applications to earth, marine and environmental sciences, pp 34 - 61, Clarendon Press, Oxford.

Janson, P., Koukkanen, M. (1999) Prototype Repository - Finite element analyses of heat transfer and temperature distribution in buffer and rock. SKB International Progress Report 01-07.

Johannes, K. (2000) Das Rückhaltevermögen alterierter Granite für endlagerrelevante Seltene Erden. Dissertation TU Clausthal. Shaker Verlag.

Kornfält, K.A, Wikman, H.(1987) Description of the map of solid rocks around Simpevarp. SKB Progress Report 25-87-02.

Kornfält, K.A., Persson, P.O. and Wikman, H. (1997) Granitoids from the Äspö area, southeastern Sweden - geochemical and geochronological data. - Geol. Fören. Stockh. Förh., 119: 109 - 114.

Le Maitre, R.W. (1979) A new generalized petrological mixing model - Contrib. Mineral. Petrol. 71: 133 - 137.

Mansfeld, J. (1991) U-Pb age determination of Småland-Värmland granitoids in Småland, southeastern Sweden. Geol. Fören. 113: 113 - 119

Markström, I. and Erlström, M. (1996) Overview of documentation of tunnel, niches and core boreholes. - SKB Progress Report HRL-96-19.

Mortimer, C.E. (1973) Chemie. Georg Thieme Verlag, Stuttgart.

Munier, R.M. (1995) Studies of geological structures at Äspö. SKB Progress Report, 25-95-21.

Prohl, H. (1996) Röntgenfluoreszenz-Untersuchung an internationalen geowissenschaftlichen Referenzproben mit Hilfe einer neu erstellten Kalibration. - Diplomarbeit TU Clausthal.

PTE (1998) Förderkonzept zur Entsorgung gefährlicher Abfälle in tiefen geologischen Formationen. Forschungszentrum Karlsruhe.

Rudnick, R.L. and Fountain, D.M. (1995) Nature and composition of the continental crust - a lower crustal perspective - Rev. Geophys. 33: 267 - 309.

Shannon, R.D. (1976) Revised effective ionic radii in halogenides and chalcogenides. Act Cryst. A32: 751-767.

Simon, K. (1990) Hydrothermal alteration of Variscan granites, southern Schwarzwald, Germany. Contrib. Mineral. Petrol. 105: 255 - 274.

SKB (1999) Deep repository of spent nuclear fuel - SR 97 - Post closure safety. SKB Technical Report TR-99-06.

Stanfors, R., Liedholm, M., Munier, R., Olsson, P. and Stille, H. (1994) Geological, structural and rock mechanical evaluation of data from tunnel section 2265-2874 m. - SKB Progress Report 25-94-18.

Stascheit, A., Knipping, B., Engelhardt, H.J., Rühe, S. and Gareis, R. (1994) In-house reference samples for geochemistry and environmental sciences. Z. dt. Geol. Gesellschaft 145: 402 - 413.

Stosnach, H. (1999) Eine Einschätzung der Verteilung von Spurenelementen in Äspö-Granitoiden und ihrer Bedeutung für die Verwendung von Graniten als geologische Barriere. Dissertation, TU Clausthal.

Streckeisen, A. (1980) Classification and nomenclature of igneous rocks - Earth Sci. Rev. 12: 1 - 33

Tuttle, O.F. (1949) Two pressure vessels for silicate-water studies. Geolog. Soc. America, Bull. 60: 1727 - 1729

Wiegand, U. (1997) Hydrogeologische Untersuchungen zu den Elementsignaturen von Grundwässern und silikatischen Gesteinen im Äspö-Granit (Schweden). Diplomarbeit, TU-Clausthal.

Acknowledgements

The research activities reported here were generously funded by the Ministry of Economics and Technology (BMWi) and were kindly supported by PtWT+E at Forschungszentrum Karlsruhe. This work would not have been possible without the generous assistance of the SKB staff at the Äspö Hard Rock Laboratory. We are especially indebted to Olle Olson, Peter Wikberg and Leif Stenberg for numerous discussions, help in field work and various underground activities.

Thanks are also due to the staff of the Department of Mineralogy, Geochemistry and Salt Deposits at the TU Clausthal: Joachim Dietrich for preparing high-quality thin sections, Klaus Herrmann for running the electron microprobe and the X-ray fluorescence analyses, Kai Schmidt and Antje Gebel for superb trace element analyses by ICP-MS.

The hydrothermal experiments were carried out at the Department of Mineralogy at the University of Hannover. Prof. François Holtz and Dieter Ziegenbein helped to set up the experimental apparatus and kindly supervised the long-term experiments.

We also wish to thank many colleagues for constructive criticism and fruitful discussions throughout the course of the project. Amongst them are: Prof. Wilhelm Johannes and Antje Wittenberg, University of Hannover; Prof. Bernd Lehmann, Alfred K. Schuster, Thomas Schirmer, and Ute Wiegand (all TU Clausthal) and Herbert Kull from GRS Braunschweig.

Appendix

A 1 Analytical and experimental procedures

A 1.1 Preparation of samples

Thin sections were cut for optical investigations and electron microprobe analyses from each sample. Powders for chemical analysis were obtained by crushing the bulk rock samples and subsequent grinding in a tungsten carbide jar to a grain-size of < 125 µm. X-ray fluorescence analyses were carried out on glass beads which were prepared by melting 600 mg of sample powder together with 3600 mg of Li-tetra-borate in Pt-vessels. Trace element determinations by inductively-coupled mass spectrometry requires dissolution of the rock powders by HF-$HClO_3$-H_2SO_4 digestion of 0.1 g sample powder in Teflon crucibles for 10 hours at 180 °C. To remove SiF_4 and all surplus acid after dissolution, the samples were evaporated to dryness under addition of HNO_3 and refilled with water to a volume of 100 ml. This results in a 1:1000 dilution of the rock.

A 1.2. Major and trace element analyses

X-ray fluorescence analysis (XRF) The main elements and some trace elements (Ba, Sr, Rb and Zr) were analyzed with a wavelength dispersive X-ray fluorescence spectrometer (Phillips PW1480) calibrated mainly with reference samples from the United States Geological Service (PROHL 1996). To check for accuracy, an in-house reference sample ('TUC-Si-G', granite, Fichtelgebirge) was measured along with the samples. The data for accuracy are summarized in Tab. A1.

Gas chromatography (GC) H_2O and CO_2 contents were analyzed by gas chromatography (GC, Fisons Instruments, Type Na 1500) calibrated by means of different organic standards. For whole rock analyses, about 5 to 8 mg of the sample material was mounted and sealed in tin capsules. Similar to RFA analyses, the in-house reference sample TUC-Si-G was analyzed for accuracy by GC. These results, too, are summarized in Tab. A1. The deviations from the certified CO_2-value are caused by the low CO_2 concentration of this sample. The value of 0.05 wt.-% is close to the detection limit of the instrument, stated by the producer as 0.02 wt.-%.

Inductively-coupled plasma mass spectrometry (ICP-MS) Trace element concentrations including REE were obtained by ICP-MS analyses (Perkin-Elmer ELAN 6000). The instrument was calibrated by means of five different solutions containing trace element concentrations within the expected range. 10 ppb of each Rh, Re and In was added to all sample solutions as an internal standard. Again, the reference sample TUC-Si-G was measured for accuracy. The data are given in Tab. A1.

Tab. A1. Accuracy (Δ [% rel.]) and precision (1σ [% rel.]) of whole-rock analyses according to the in-house reference standard 'TUC-Si-G'. Reference values from Stascheit *et al.* (1994).

Wt.-%	Reference	Measured	Δ [%]	1 σ [%]	ppm	Reference	Measured	Δ [%]	1 σ [%]
SiO_2	68.3	68.7	+ 0.6	± 0.26	Rb	220	239	+ 8.6	± 1.9
TiO_2	0.52	0.52	-	± 0.83	Ba	791	801	+ 1.3	± 1.8
Al_2O_3	15.6	15.2	- 2.4	± 0.17	Sr	211	216	+ 2.4	± 1.2
Fe_2O_3	3.17	3.14	- 1.0	± 1.01	Y	23.0	22.9	- 0.40	± 12.1
MnO	0.05	0.05	-	± 8.25	Zr	217	209	- 3.7	± 11.0
MgO	0.80	0.88	+ 10.0	± 2.03	Li	91.0	92.4	+ 1.5	± 4.0
CaO	1.70	1.79	+ 5.3	± 5.60	Cs	13.0	12.0	- 3.8	± 2.2
Na_2O	3.42	3.40	- 0.66	± 0.92	Co	7.0	5.6	- 20	± 5.7
K_2O	4.93	4.86	- 1.4	± 0.17	La	54.0	52.4	- 3.0	± 17.7
P_2O_5	0.30	0.32	+ 6.7	± 2.57	Ce	108.0	109.8	+ 1.7	± 5.2
H_2O	1.33	1.44	+ 838	± 10.78	Pr	11.0	11.1	+ 0.91	± 12.9
CO_2	0.04	0.05	+ 25.0	± 4.81	Nd	46.0	39.3	- 14.6	± 11.6
					Sm	8.1	6.4	- 21	± 9.7
					Eu	1.2	1.1	- 8.3	± 9.5
					Gd	5.9	5.6	- 5.1	± 7.8
					Tb	1.0	0.8	- 20	± 5.5
					Dy	4.1	3.0	- 27	± 35.3
					Ho	0.8	1.0	+ 25	± 33.7
					Er	2.1	2.2	+ 4.8	± 6.3
					Tm	0.3	0.3	-	± 2.3
					Yb	2.0	2.0	-	± 2.0
					Lu	0.3	0.3	-	± 2.4
					Hf	5.5	5.7	+ 3.6	± 12.0
					Th	31.0	22.5	- 27	± 40.4
					U	7.1	7.8	+ 9.9	± 17.9

Mineral analysis Major elements of rock-forming minerals were analyzed using a CAMECA SX-100 electron microprobe at TUC. Within a thin section, at least three representative grains of each mineral species were analyzed. The number of measurements per mineral species was ≥ 12. The composition of both feldspars was analyzed by line-scans of 20 to 40 single points. The instrument was calibrated by means of natural mineral standards. For further details concerning counting times and data processing see Stosnach (1999).

A 2 Petrography of granites

Conventionally, the modal composition of the leucocratic components in granitic rocks are plotted in quartz - alkali feldspar - plagioclase diagrams developed by Streckeisen (1980). Such diagrams are usually based on optical point-counting statistics obtained from petrographic analyses in thin section. If, however, whole-rock major element and microprobe data on the constituent minerals are available as is the case in this study, a normative modal composition is preferable to point-counting data. The normative method allows a calculation of modal data obtained for coarse-grained rocks that is more precise than the point-counting method. The results of this type of petrographic characterization are given in Fig. A1.

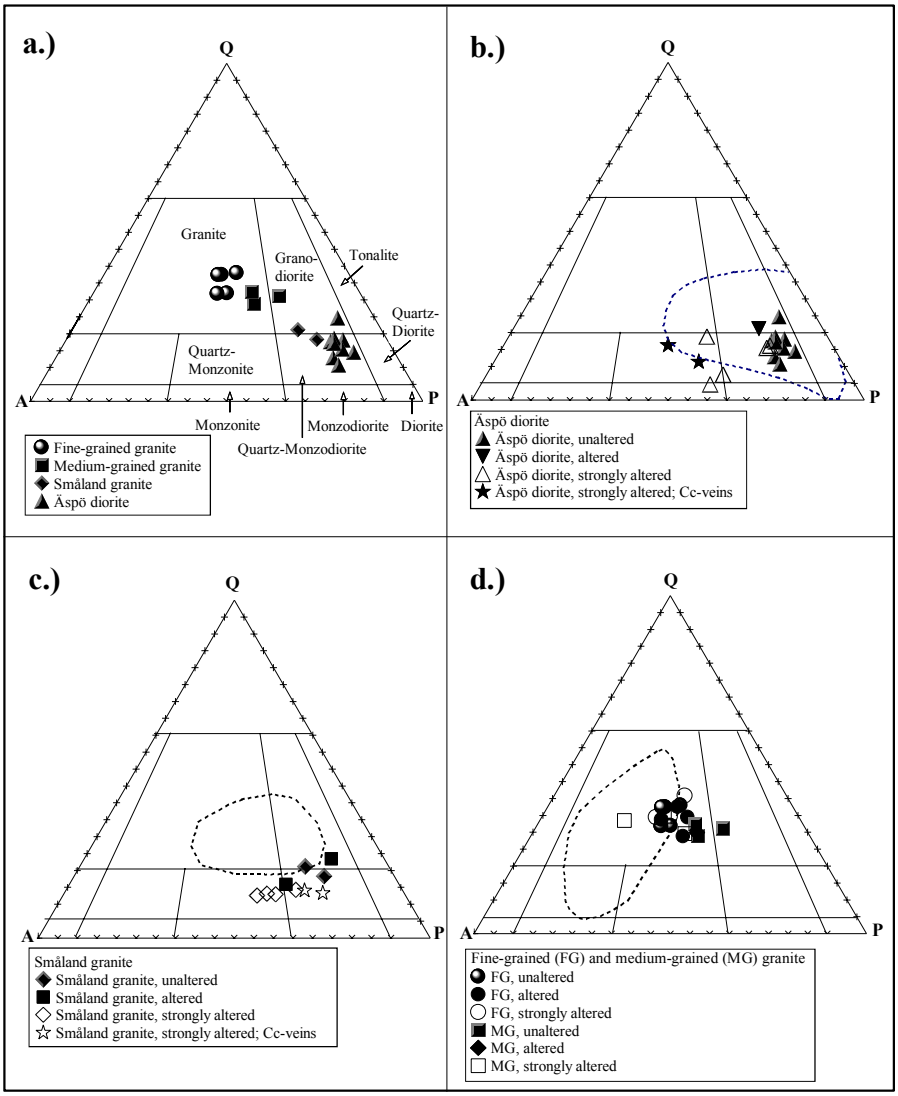

Fig. A1: Composition of Äspö granitoids as normative proportions of quartz, alkali feldspar and plagioclase in triangular diagrams following Streckeisen (1980). Dashed lines include the compositional ranges obtained by Kornfält et al. (1997).

Normative compositions of the whole-rock samples have been calculated utilizing the algorithm developed by Le Maitre (1979), which is based on a least-squares-fit calculation employing bulk rock and major mineral element data. A disadvantage of this method is that

the amounts of accessory phases like rutile cannot be calculated sufficiently well.

In altered granites, feldspar minerals are largely present only in the form of pseudomorphs after primary grain images. In addition, a slight foliation is found in the Äspö granitoids, which will result in an overestimation of minerals preferentially oriented along structural features. Such differences become clear when the normative mineral abundances calculated here are compared with the results of point-counting analyses presented by Kornfält et al. (1997). Their modal analyses have probably overestimated the alkali feldspar components in most Äspö granitoids (see Fig. A1c and A1d).

The most frequent rock type in the Äspö area is the Äspö Diorite, which can be classified as quartz monzodiorite and granodiorite by modal analysis (Fig. A1.b.). This rock type is dark reddish to gray in color and contains megacrysts of K-feldspar with grain-sizes of 10-30 mm or pseudomorphs after K-feldspar. The main minerals (in vol.-%) are plagioclase (32-58), K-feldspar (7-32), quartz (3-20), biotite/chlorite (8-19) and epidote (2-13). In five samples hornblende is present with up to 19 vol.-% and titanite occurs in almost all samples in amounts of 1-3 vol.-%. Småland Granite is less abundant when compared to Äspö Diorite. It differs macroscopically from the Äspö Diorites in its more reddish color and the less frequent K-feldspar megacrysts. In addition, the Småland Granites (Fig. A1.c.) are richer in quartz (9-14 vol.-%) and K-feldspar (14-29 vol.-%). The modal amounts of plagioclase (15-49 vol.-%), biotite/chlorite (9-20 vol.-%), epidote (1-15 vol.-%) and titanite (1-3 vol.-%) are in the same range as those of Äspö Diorites. Hornblende contents are small with 1-3 vol.-% (present in only two samples). In many places the Äspö Diorite is cut by the Småland Granite. However, according to radiometric datings (Kornfält *et al*. 1997, Mansfeld 1991) the age differences between Äspö Diorite (1804 ± 3 Ma) and Småland Granite (1800 ± 20 Ma) are insignificant and a common intrusion of both magma-types is probable.

The reddish Fine- and Medium-grained Granites occur rather frequently both as small irregular intrusions or dikes, veins and patches, often cutting the other two granitoid types. They are assumed to be slightly younger when compared to Äspö Diorite and Småland Granite: Radiometric datings by Kornfält *et al*. (1997) resulted in ages of 1794 (+16/-12) and 1808 (+33/-30) Ma, respectively. The Fine- and Medium-grained Granites are in most cases rich in quartz (25-38 vol.-%), plagioclase (21-40 vol.-%) and K-feldspar (19-42 vol.-%) with comparatively low contents of biotite/chlorite (1-9 vol.-%), epidote (0.5-8 vol.-%) and titanite (max. 1.2 vol.-%). With one exception they can be classified as true granites according to modal analyses (Fig. A1.d.).

A 3 Major and trace element data for granitoids

Tab. A2: Representative whole rock analyses of fresh and altered samples of Äspö granitoids

		Äspö Diorite		Småland Granite		Fine-/Medium-grained Granite	
		fresh	altered	fresh	altered	fresh	altered
		Äspö15	Äspö17	SG01AT	SG02AT	Äspö14	Äspö09
SiO_2	[wt.-%]	58.14	59.55	59.94	59.22	75.16	76.14
TiO_2	[wt.-%]	0.88	0.83	0.80	0.83	0.07	0.10
Al_2O_3	[wt.-%]	17.94	17.47	17.06	16.96	13.45	12.77
Fe_2O_3	[wt.-%]	5.80	5.25	5.08	5.14	0.69	0.93
MnO	[wt.-%]	0.10	0.07	0.10	0.10	0.02	0.02
MgO	[wt.-%]	2.46	2.31	2.46	2.35	0.11	0.21
CaO	[wt.-%]	5.08	4.61	4.11	4.28	0.95	0.69
Na_2O	[wt.-%]	4.23	4.13	4.33	4.18	3.17	3.04
K_2O	[wt.-%]	3.28	2.80	3.40	4.24	5.84	5.53
P_2O_5	[wt.-%]	0.39	0.35	0.36	0.37	0.04	0.05
H_2O	[wt.-%]	1.65	3.78	1.44	2.52	0.14	0.60
CO_2	[wt.-%]	0.26	0.39	0.18	0.22	0.33	0.11
Ba	[µg/g]	1967	1675	1432	1357	258	264
Sr	[µg/g]	1364	1261	1056	1312	127	100
Rb	[µg/g]	105	95	109	179	226	253
Li	[µg/g]	49	39	32	23	7.3	16
Co	[µg/g]	26	23	23	18	36	60
Th	[µg/g]	6.8	6.1	13.1	12.7	20.8	39.9
U	[µg/g]	2.2	1.9	4.8	4.6	23.1	21.4
Y	[µg/g]	31.8	20.9	22.2	23.4	18.4	27.0
Cs	[µg/g]	1.4	0.9	2.0	1.6	1.3	1.1
La	[µg/g]	55.0	48.9	66.5	61.5	19.2	25.6
Ce	[µg/g]	127	117	130	126	37.1	54.3
Pr	[µg/g]	14.8	13.3	14.1	13.7	4.1	5.9
Nd	[µg/g]	57.7	51.7	51.8	51.5	14.5	20.7
Sm	[µg/g]	8.6	7.7	7.8	7.8	2.7	3.8
Eu	[µg/g]	1.5	1.2	1.9	1.8	0.3	0.4
Gd	[µg/g]	6.8	6.2	8.5	8.4	2.5	3.6
Tb	[µg/g]	0.9	0.8	0.8	0.8	0.5	0.7
Dy	[µg/g]	5.0	4.5	4.5	4.5	3.3	4.8
Ho	[µg/g]	0.8	0.7	0.8	0.8	0.7	1.1
Er	[µg/g]	2.3	2.1	2.1	2.2	2.1	3.2
Tm	[µg/g]	0.3	0.3	0.3	0.3	0.4	0.6
Yb	[µg/g]	2.1	1.9	1.8	1.9	2.5	4.1
Lu	[µg/g]	0.3	0.3	0.3	0.3	0.4	0.6

Tab. A3: Average and compositional range (std. deviation from the mean, 1 σ) of Äspö granitoids

		Äspö Diorite	1 σ	Småland Granite	1 σ	Fine-/Medium-grained Granite	1 σ
SiO_2	[wt.-%]	58.41	0.36	58.68	0.51	72.57	0.72
TiO_2	[wt.-%]	0.85	0.01	0.83	0.03	0.24	0.04
Al_2O_3	[wt.-%]	17.40	0.17	17.11	0.19	13.93	0.21
Fe_2O_3	[wt.-%]	5.64	0.12	5.32	0.22	1.79	0.23
MnO	[wt.-%]	0.09	<0.01	0.09	<0.01	0.03	<0.01
MgO	[wt.-%]	2.41	0.07	2.38	0.11	0.55	0.10
CaO	[wt.-%]	4.55	0.22	4.63	0.54	1.47	0.21
Na_2O	[wt.-%]	4.31	0.12	4.45	0.12	3.32	0.09
K_2O	[wt.-%]	3.48	0.19	3.32	0.16	5.19	0.19
P_2O_5	[wt.-%]	0.36	<0.01	0.35	<0.01	0.09	<0.01
H_2O	[wt.-%]	2.72	0.43	3.37	0.27	0.62	0.11
CO_2	[wt.-%]	0.65	0.14	0.72	0.28	0.30	0.05
Ba	[µg/g]	1789	130	1453	90	745	112
Sr	[µg/g]	1130	80	1069	76	375	63
Rb	[µg/g]	133	10	148	10	193	17
Li	[µg/g]	39	3	42	5	23	4
Co	[µg/g]	24	1	20	2	29	5
Th	[µg/g]	7.8	0.5	9.5	0.9	26.3	3.0
U	[µg/g]	2.9	0.4	4.2	0.3	11.7	1.9
Y	[µg/g]	25.2	1.7	19.6	1.0	20.5	2.2
Cs	[µg/g]	1.5	0.2	1.7	0.3	2.1	0.3
La	[µg/g]	51.5	3.0	50.0	3.1	37.6	3.5
Ce	[µg/g]	122	4	113	6	82	8
Pr	[µg/g]	14.5	0.6	13.3	0.6	8.5	0.8
Nd	[µg/g]	55.7	2.0	50.0	2.5	28.7	2.7
Sm	[µg/g]	8.3	0.3	7.5	0.4	4.7	0.5
Eu	[µg/g]	1.62	0.08	1.48	0.10	0.54	0.08
Gd	[µg/g]	6.6	0.3	6.3	0.4	4.2	0.4
Tb	[µg/g]	0.92	0.04	0.80	0.03	0.68	0.06
Dy	[µg/g]	4.94	0.20	4.26	0.16	3.89	0.42
Ho	[µg/g]	0.83	0.04	0.77	0.02	0.79	0.08
Er	[µg/g]	2.31	0.11	2.11	0.06	2.28	0.25
Tm	[µg/g]	0.33	0.02	0.31	<0.01	0.37	0.05
Yb	[µg/g]	2.17	0.10	2.03	0.06	2.57	0.32
Lu	[µg/g]	0.30	<0.01	0.30	<0.01	0.38	0.05

A 4 Hydrothermal experiments

In order to allow reactions of natural epidote material with REE-dotated fluids under controlled conditions, hydrothermal experiments have been conducted in conventional hydrothermal pressure apparatus. This experimental technique was first described by Tuttle (1949) and has only slightly been modified ever since. The experimental set-up used here is shown in Fig.A2.

It consists of an electrically heated oven which contains a cold-seal internal pressure vessel. The pressure is set up and maintained by controlled heating of a specific volume of water. Temperatures are controlled by a Cr/Cr-Ni thermocouple fixed on top of the pressure vessel close to the sample capsule. Individual sample capsules were prepared from gold tubes (4.4 mm in diameter). Each capsule was filled with ca. 50 mg of the solid epidote material and ca. 50 mg of trace element-enriched solution and was subsequently sealed by welding. During the experiments, pressures and temperatures were kept constant at a range of ± 0.5 MPa and ± 10^{o}C, respectively. No fluid or mass loss was observed after rapid quenching of the capsule to room temperature at the end of each experiment.

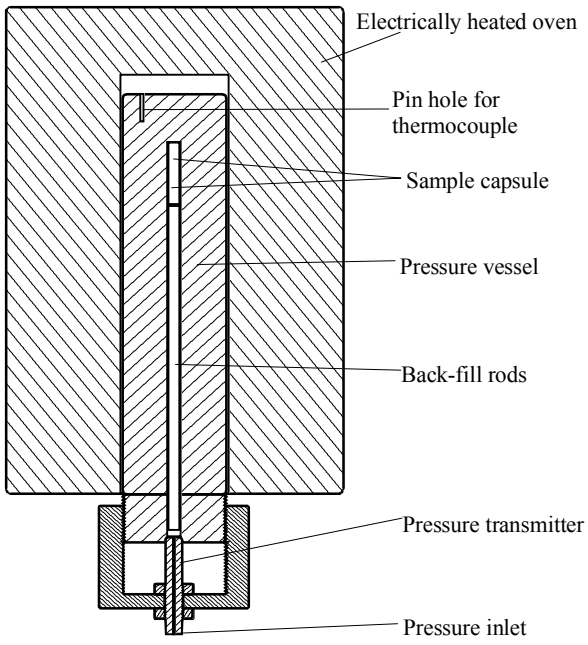

Fig. A2: Set-up for hydrothermal experiments conducted on epidote/solute reactions.

From the HRL-tunnel no epidote was available in significant quantities and sufficient purity to be used as starting material in the hydrothermal experiments. Underground waters sampled from the tunnel have been found to contain very low concentrations of REE, Th and U (Wiegand 1997). Thus, a natural gem-quality epidote crystal was crushed to a grain size of < 63 µm and artificial solutions were prepared containing higher amounts of the required elements. The composition of epidote starting material was analyzed by electron microprobe and ICP-MS analyses. The major and trace element contents of the epidote and the dotated solutions are given in Tab. A4 and the epidote REE pattern is shown diagramatically in Fig.

A3. A comparison with the artificially enriched experimental solutions makes it clear that the trace element contents of the natural epidote are negligible and, thus, will not have any significant effect on the exchange reactions.

After the experiments, the capsules were opened carefully to avoid any loss of solid or fluid. The experimental products were filtered (0.2 μm pore) in order to separate the solid run products from the coexisting solutions. The solid run products were analyzed by ICP-MS for its trace element contents after dissolution by HF-$HClO_4$. Likewise, the filtered liquids were diluted and analyzed for their trace element contents by ICP-MS.

Tab. A4: Major and trace element concentrations of epidote and artificially enriched solutions used in hydrothermal experiments. MELK stands for artificially enriched solutions

Wt.-%	Epidote	ppm	Epidote	MELK-5	MELK-9
SiO_2	36.0	La	1.5	1000	10000
TiO_2	0.1	Ce	3.0	1000	10000
Al_2O_3	21.8	Nd	7.8	1000	10000
FeO^t	13.7	Eu	1.6	1000	10000
MnO	0.2	Yb	2.8	1000	10000
MgO	0.2	Y	28.3	1000	10000
CaO	22.6	Th	0.4	10	1000
Na_2O	0.01	U	7.0	10	1000
K_2O	0.01				

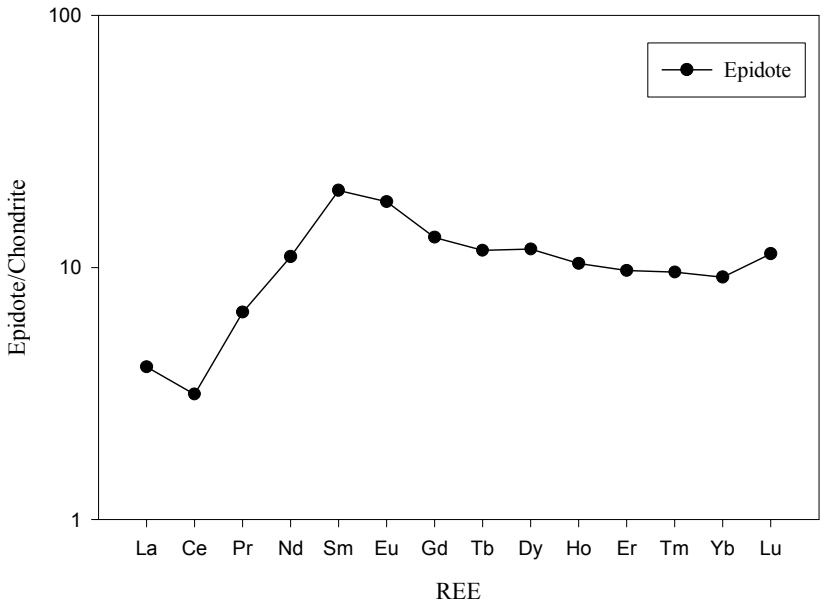

Fig. A3: Chondrite-normalized REE pattern for epidote used in hydrothermal experiments

Tab. A5: Experimental details of representative runs using the enriched solution MELK-9 (10000 ppm of each element, except Th and U, which are present in a concentration of 1000 ppm). Analyses of trace elements in run products (solids and solutions) obtained by ICP-MS.

Run-Nr..	KEN-37 Solid	KEN-37 Solution	KEN-38 Solid	KEN-38 Solution
Capsule	Au	Au	Au	Au
Sample (mg)	0.0534	0.0534	0.0514	0.0514
Solution (mg)	0.0576	0.0576	0.0582	0.0582
T/P	550°C/50 MPa	550°C/50 MPa	450°C/50 MPa	450°C/ MPa
Duration from	09.06.99 12.00 h	09.06.99 12.00 h	30.06.99 12.00 h	30.06.99 12.00 h
to	16.06.99 12.00 h	16.06.99 12.00 h	07.07.99 12.00 h	07.07.99 12.00 h
			ppm	
Y	8567	51	6472	2147
La	8811	46	7631	1226
Ce	9154	11	8998	166
Nd	9216	51	7635	1631
Eu	8074	57	6303	1828
Yb	8620	28	8620	29
Th	998	0.10	998	0.11
U	851	0.2	687	163

Run-Nr.	KEN-40 Solid	KEN-40 Solution	KEN-45 Solid	KEN-45 Solution
Capsule	Au	Au	Au	Au
Solid (mg)	0.0519	0.0519	0.0514	0.0514
Solution (mg)	0.0566	0.0566	0.0567	0.0567
T/P	350°C/50 MPa	350°C/50 MPa	250°C/50 MPa	250°C/50 MPa
Duration from	04.08.99 12.00 h	04.08.99 12.00 h	07.07.99 12.00 h	07.07.99 12.00 h
to	11.08.99 12.00 h	11.08.99 12.00 h	04.08.99 12.00 h	04.08.99 12.00 h
		ppm		
Y	5077	3542	611	8008
La	3575	5282	270	8587
Ce	9147	18	9069	96
Nd	4739	4528	343	8923
Eu	4214	3916	444	7687
Yb	8391	257	2434	6215
Th	997	0.224	997	0.187
U	687	164	765	86